Science of the Total Environment 951 (2024) 174996

Contents lists available at ScienceDirect

Science of the Total Environment

journal homepage: www.elsevier.com/locate/scitotenv

A multidisciplinary approach using hydrogeochemistry, $\delta^{15}N_{NO3}$ isotopes, land use, and statistical tools in evaluating nitrate pollution sources and biochemical processes in Costa Rican volcanic aquifers

Helga Madrigal-Solís [a,*], Iñaki Vadillo-Pérez [b], Pablo Jiménez-Gavilán [b], Alicia Fonseca-Sánchez [a], Luis Quesada-Hernández [a], Hazel Calderón-Sánchez [a], Alicia Gómez-Cruz [a], Jorge Herrera Murillo [c], Roy Pérez Salazar [d]

[a] Programa de Hidrología Ambiental, Escuela de Ciencias Biológicas, Universidad Nacional, 40101, Heredia, Costa Rica
[b] Grupo de Hidrogeología, Departamento de Ecología y Geología, Universidad de Málaga, 29016 Málaga, Spain
[c] Laboratorio de Análisis Ambiental, Escuela de Ciencias Ambientales, Universidad Nacional, 40101, Heredia, Costa Rica
[d] Laboratorio de Gestión de Desechos y Aguas Residuales (LAGEDE), Escuela de Química, Universidad Nacional, 40101, Heredia, Costa Rica

HIGHLIGHTS

- Long-term monitoring (2015–2022) revealed critical NO_3^- groundwater contamination from wastewaters and N-fertilizers.
- Cost-effective methodology proposed, with and without the use of $\delta^{15}N_{NO3}$ isotopes.
- Integrated socio-economic parameters, hydrogeochemistry, $\delta^{15}N_{NO3}$ isotopes, land use, and statistical methods.
- Indicated similar nitrate impacts from urban and agricultural zones, revising previous underestimations.
- Emphasized the importance of challenging traditional Bayesian mixing models with a holistic approach.

GRAPHICAL ABSTRACT

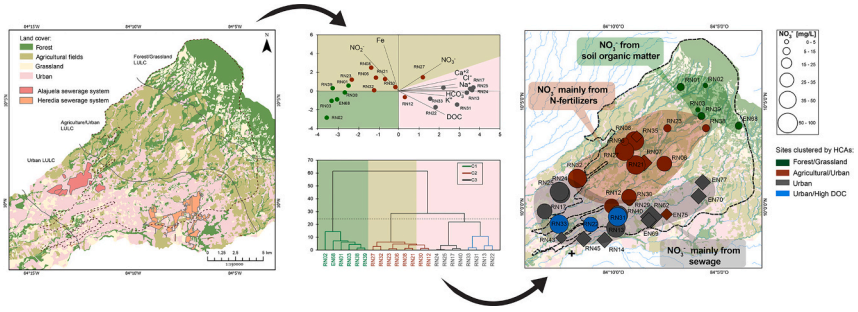

ARTICLE INFO

Edited by: Jurgen Mahlknecht

Keywords:
Agriculture
Wastewater
Groundwater
Dissolved organic carbon
Nitrification
Hierarchical cluster analysis

ABSTRACT

Nitrate pollution threatens the Barva and Colima multi-aquifer system, the primary drinking water source in the Greater Metropolitan Area of Costa Rica. In addressing nitrate contamination dynamics, this study proposes an integrated approach by combining multivariate statistical analyses, hydrochemical parameters, sewage discharge, and regional land-use and land-cover patterns to assess the extent and degree of contamination, dominant biogeochemical processes, and refine the interpretation of nitrate sources previously derived solely from $\delta^{15}N_{NO3}$ information. Over seven years (2015–2022), 714 groundwater samples from 43 sites were analyzed for nitrate and major ions, including two sampling campaigns for dissolved organic and inorganic carbon, nitrite, ammonium, Fe_{Total}, Mn_{Total}, and $\delta^{15}N_{NO3}$ analyses. The findings presented elevated nitrate concentrations in urban and agricultural/urban areas, surpassing the Maximum Concentration Levels on several occasions, and oxidizing conditions favoring mineralization and nitrification processes in unconfined Barva and locally confined Upper Colima/Lower Colima aquifers. Similar nitrate contents and spatial patterns in agricultural and urban

* Corresponding author.
E-mail address: helga.madrigal.solis@una.ac.cr (H. Madrigal-Solís).

https://doi.org/10.1016/j.scitotenv.2024.174996
Received 2 February 2024; Received in revised form 12 July 2024; Accepted 21 July 2024
Available online 25 July 2024

zones in the shallow Barva aquifer suggest comparable contributions from nitrogen fertilizers and urban wastewaters despite the gradual increase in urban land cover and the reduction of agricultural areas. Isotopic analyses and dissolved organic carbon (DOC) indicate a shift in nitrate sources from agricultural to urban areas in both Barva and Colima aquifers. Principal Component and Hierarchical Cluster Analyses link land use, nitrate sources, and water quality. Three distinct sample clusters aligned with forest/grassland, agricultural/urban, and urban land use, emphasizing the impact of anthropogenic activities on groundwater quality, even in the deeper Colima aquifers. The study challenges nitrate isotope mixing models, enhancing accuracy in identifying pollution sources and assessing the spatial extent of contamination by incorporating DOC and other hydrochemical parameters. Similar outcomes, with and without the use of nitrate isotopes, reinforce the usefulness of the integrated approach, providing a practical and cost-effective alternative.

1. Introduction

Nitrate (NO_3^-) contamination in groundwater is a global problem mainly caused by human-related activities (Abascal et al., 2022). Agricultural practices, such as the application of livestock waste and nitrogen-based fertilizers, and sewage leaks are major sources of nitrate pollution (Minet et al., 2017; Shen et al., 2023; Vystavna et al., 2017; Zaryab et al., 2022). In the subsurface, nitrogen (N) compounds undergo adsorption, biochemical and chemical transformations, and leaching into groundwater (Kendall et al., 2007). Organic N compounds serve as a source of carbon and nutrients for mineralizing bacteria, releasing ammonium (NH_4^+). Then, nitrifying bacteria oxidize NH_4^+ originating from organic matter (OM) or ammoniacal fertilizers, into nitrite (NO_2^-), and then into NO_3^-, particularly in oxidizing conditions (Utom et al., 2020), increasing NO_3^- levels in groundwaters (Kendall, 1998). Denitrification, mainly conducted by bacteria, reduces NO_3^- into NO_2^-, which is then converted to gaseous N (N_2), both in oxic or anoxic conditions (Ji et al., 2015; Utom et al., 2020), lowering NO_3^- concentrations (Jurado et al., 2017; Nikolenko et al., 2018).

In regional aquifer systems, the most dependable approach for identifying the distribution of redox processes is by assessing the depletion of soluble electron acceptors and the formation of distinct by-products along the groundwater flow path (McMahon and Chapelle, 2008). Subsurface microorganisms prefer dissolved oxygen (DO) as an electron acceptor due to its high energy yield, followed by NO_3^-, manganese (IV) [Mn(IV)], ferric iron [Fe (III)], sulfate (SO_4^{2-}), and carbon dioxide (CO_2) in the absence of oxygen (McMahon and Chapelle, 2008; Nikolenko et al., 2018). Assessing dissolved organic carbon (DOC), dissolved inorganic carbon (DIC), and various N species also contribute to the evaluation of redox conditions and nitrification/denitrification processes impacting NO_3^- levels in groundwater (Gao et al., 2021; Zuo et al., 2021). Favorable redox conditions, with appropriate DO levels and low Fe^{+2} and Mn^{+2} concentrations, facilitate nitrification (Utom et al., 2020). When analytical information on Fe(II) and Mn(II) reduced forms is unavailable, Fe_{total} and Mn_{total} can also indicate redox conditions (He et al., 2022).

The use of a multidisciplinary approach, combining hydrochemistry, NO_3^- stable isotopes ($\delta^{15}N_{NO3}$), land-use and land-cover (LULC) analyses, and multivariate statistical techniques have also contributed to the assessment of NO_3^- pollution dynamics in groundwater (Hauptman et al., 2023; Huang et al., 2022; Knoll et al., 2019; Liu et al., 2021). The presence of chloride (Cl^-), potassium (K^+), sodium (Na^+), NH_4^+, bicarbonate (HCO_3^-), and NO_3^- resulting from the decomposition of farm animal wastes and septic tank effluents can serve as indicators of organic contamination sources when levels exceed natural concentrations (Ben Messaoud et al., 2021; Minet et al., 2017; Robertson, 2021). Since many of these components are also present in fertilizers, the application of hydrochemical relations and molar ratios have contributed to the differentiation of primary NO_3^- sources (Subba Rao et al., 2022; Minet et al., 2017). N isotopes are also useful for identifying NO_3^- origins and detecting nitrification, denitrification, and dilution in groundwater (Aravena et al., 1993; Aravena and Robertson, 1998; Harris et al., 2022; Torres-Martínez et al., 2021; Kendall, 1998). Other common tools include correlation matrices and multivariate statistical analyses (Torres-Martínez et al., 2021). These analyses facilitate the integration of data from isotopic and hydrochemical parameters. Principal Component Analysis (PCA) (Gan et al., 2022; Huang et al., 2022, 2018) and Hierarchical Cluster Analysis (HCA) (Liu et al., 2021), incorporate a broader range of parameters enhancing the identification of pollution sources.

Despite their abundant water resources, tropical regions like Costa Rica rely heavily on groundwater for drinking supplies due to surface water contamination (Bower, 2014). The aquifers in the Central Valley, such as the Barva and Colima, supply drinking water to 60-90% of the Greater Metropolitan Area (GAM) (Bower, 2014; Reynolds-Vargas et al., 2006; SINIGIRH, 2018), projected to reach 2.7 million people by 2025 (INEC, 2018). However, NO_3^- contamination has significantly impacted groundwater quality in these aquifers (Reynolds-Vargas et al., 2006; Mora-Alvarado et al., 2017; Madrigal-Solís et al., 2017, 2019, 2022). Recent studies showed NO_3^- values exceeding regulatory limits in the shallow Barva aquifer, with ongoing contamination in the Upper Colima aquifer, and emerging pollution in the discharge zone of the deeper Lower Colima aquifer (Madrigal-Solís et al., 2022). In 2004, NO_3^- isotopic analyses indicated that NO_3^- in the Barva aquifer was primarily derived from sewage and fertilizers due to urban expansion and intensive agriculture (Reynolds-Vargas et al., 2006). By 2019, a dual NO_3^- isotope approach and a Bayesian mixing model attributed a minor portion of NO_3^- to N-fertilizers (Sánchez-Gutiérrez et al., 2023), despite continued intensive agricultural practices (Madrigal-Solís et al., 2019).

Regardless of their convergence capabilities (Cao et al., 2022; He et al., 2022; Marković et al., 2022; Torres-Martínez et al., 2021), traditional and Bayesian dual nitrate isotope mixing models may introduce substantial uncertainties (Zhang et al., 2020, 2018). Unreliable outcomes may arise due to important overlapping $\delta^{15}N_{NO3}$ signatures between NH_4^+ fertilizers, SON, sewage, and manure, isotopic fractionation, and mixing of isotopic signatures from multiple NO_3^- sources (Choi et al., 2017; Kendall et al., 2007; Minet et al., 2017; Xue et al., 2009). Combining NO_3^- isotopes with hydrochemistry, redox indicators, LULC information, and multivariate techniques can improve the identification and verification of the primary NO_3^- sources and processes (Gupta and Kumari, 2023; Torres-Martínez et al., 2020).

Given the complexity of NO_3^- pollution in the Barva and Colima aquifers, which supply nearly 2 million people in Costa Rica, this research aims to (a) evaluate the extent of NO_3^- contamination along flow paths through a long-term hydrochemical monitoring network (2015 to 2022), (b) identify dominant processes like mineralization, nitrification, and denitrification, (c) assess the influence of sewage, N-fertilizers, and soil OM on groundwater quality across LULC patterns, and (d) propose a practical approach to identify NO_3^- sources using DOC and other indicators for regions with limited $\delta^{15}N_{NO3}$. This comprehensive approach to diverse sources of NO_3^-, DOC, and varied biogeochemical processes is essential for identifying the impact of agricultural practices and inadequate wastewater management on NO_3^- contamination, supporting effective control measures within the integrated water resources management framework in the northern sector of the Central Valley of Costa Rica.

For the first time in this area, this study applies a multidisciplinary approach combining $\delta^{15}N_{NO3}$, DOC, DIC, NH_4^+, NO_2^-, Fe_{total}, Mn_{total}, DO,

Eh, major ions, and LULC assessments to understand NO_3^- contamination dynamics and biogeochemical processes affecting groundwater quality in Barva, Upper Colima, and Lower Colima aquifers. This methodology, emphasizing DOC, correlation matrices, and multivariate statistical techniques, aims to generate the first zonation of major NO_3^- sources within the study area, without relying solely on N isotopic information. The innovative aspect also lies in its comprehensive approach to verify NO_3^- sources, previously assessed only through a Bayesian mixing model, given the large uncertainties associated with such models. The scarcity of literature validating these models with hydrochemical data in volcanic aquifers emphasizes the significance of this proposed methodology for refining the relative importance of main pollutant sources in Costa Rican volcanic aquifers.

2. Study area

The study area in central Costa Rica, between 9°57′31″-10°8′1" N latitude and 84° 3′44'-84°15′17" W longitude, includes four volcanic aquifers within the Barva and Colima multi-aquifer system (Fig. 1a). The region has a rainy season from May to mid-December, with peaks in May–June and August–October and a dry season from mid-December to April (Magaña et al., 1999; Maldonado et al., 2013). Annual precipitation varies with altitude, from 3030 mm in high-altitude areas to 1960 mm in low-altitude areas (IMN, 2014). Temperatures in the low-altitude areas range from 20 to 24 °C and are about 10 °C in high-altitude areas (IMN, 2014). Andisols cover 73 % of the area, while Ultisols and Inceptisols cover 3.5 %, with the remainder urbanized (IICA et al., 2017). The middle zone has been characterized by intensively managed coffee plantations (Madrigal-Solís et al., 2014, 2019), with at least three annual fertilizer applications including NPK, magnesium (Mg^{2+}), and 90 kg/ha of urea in May and August, and 225 kg/ha of ammonium nitrate (NH_4NO_3) in November (Castro-Tanzi et al., 2012; ICAFE, 2020). By 2020, only 14 % of the population in the country was connected to a sewerage system with treatment, 8 % was connected to a sewerage system lacking treatment, and 76 % to septic tanks (Mora-Alvarado and Portuguez, 2021). Urban sanitation systems, especially in Heredia and Alajuela, are limited, with many residents relying on septic tank systems (Bower, 2014; MINAE, 2023).

2.1. Geology and petrographic composition

In the central region of Costa Rica, lava flows were extruded from fissures or the stratovolcano craters of the Central Volcanic Cordillera (BGS/SENARA, 1988). The Valle Central (Central Valley) comprises a Tertiary sedimentary bedrock overlaid by Quaternary lava and lava breccias, interspersed with pyroclastic material like tuffs and ignimbrites. The study area includes the Colima, Tiribí, and Barva Formations (Fig. 1a), with aquifers in the fractured lavas and lava breccias of the Lower Colima, Upper Colima, Bermúdez, Los Ángeles, and Bambinos Members (BGS/SENARA, 1988; Echandi, 1981). The felsic lavas and breccias in the Lower Colima Member consist of trachyandesites and porphyritic andesites, with anorthite plagioclase phenocrystals. The Puente Mulas Member includes tuffs and ignimbrites, while the Upper Colima Member lavas and lava breccias are aphyric andesites with plagioclase phenocrystals (Table S1) (Kussmaul, 1988). The Tiribí Formation consists of chemically diverse felsic tuff and ignimbrites, including andesites transitioning to shoshonitic dacites (Kussmaul, 1988; Kussmaul and Sprechmann, 1982), basaltic-andesites, trachytes, and trachydacites (Hannah et al., 2002). The younger lavas of the Barva Formation are more mafic than those in the Colima Formation (Pérez et al., 2006). The Bermúdez Member lavas are fractured porphyritic basaltic andesites with plagioclase and anorthite phenocrysts (Echandi, 1981; Arredondo Li and Soto, 2007) (Table S1). The Los Bambinos Member lavas are porphyritic andesites, with plagioclase phenocrysts (Arredondo Li and Soto, 2007), while the Los Angeles Member lavas are basaltic andesitic, with a porphyritic aphanitic texture (Arredondo Li and Soto, 2007; Rojas et al., 2017) (Table S1).

2.2. Hydrogeology

The Barva and Colima multi-aquifer system comprises the Lower Colima, Upper Colima, Lower Barva, and Upper Barva aquifers (Los Ángeles and Los Bambinos sub aquifers) (Protti, 1986; Ramírez Ch. and Alfaro M., 2002) (Fig. 1a). The Lower Colima is locally confined and semiconfined beneath the Upper Colima, recharging through vertical percolation from the Upper Colima and direct infiltration when not confined (TAHAL, 1990; Arias-Salguero et al., 2006; Madrigal-Solís et al., 2022). In the Colima aquifers, groundwater flows from NE to SW (Fig. 1e and Supplementary Fig. S1b-c). The Upper Colima aquifer is confined and semiconfined when underlying the Barva aquifer and Tiribí Formation. Due to the relatively high hydraulic connectivity with the Barva aquifer through the Tiribí Formation (BGS/SENARA, 1988; Arias-Salguero et al., 2006), the Upper Colima partially recharges from the Barva aquifer (Madrigal-Solís et al., 2022).

The fractured lavas and lava breccias from the Colima and Barva aquifers present porosities from 0.05 to 0.25 % (Foster et al., 1985), with the Barva aquifer exhibiting high permeability (1–10 m/day) (Ramírez Ch. and Alfaro M., 2002). Groundwater in the Lower Barva aquifer flows from NE to SW, covers 190 km^2 (Fig. 1d, Supplementary Fig. S1a), and recharges from the Upper Barva, direct infiltration, and influent rivers, while the Upper Barva primarily recharges through direct infiltration (BGS/SENARA, 1988; Gómez-Cruz, 1987; Madrigal-Solís et al., 2022; Reynolds-Vargas and Fraile-Merino, 2009).

Tuffs and ignimbrites of the Tiribí and Puente Mulas units (Fig. 1a) act as aquitards, partially separating the Colima and Lower Barva aquifers and allowing vertical water exchange (BGS/SENARA, 1988; Foster et al., 1985; Losilla et al., 2001). These aquitards have permeability values ranging from 1,16 to 2.72×10^{-4} m/day (Ramírez Ch. and Alfaro M., 2002), high transmissivities (1000–5000 m^2/d), porosities of 0.45 to 0.60 %, and very high groundwater flow velocities (Foster et al., 1985; Losilla et al., 2001). Pyroclasts, debris flow lahars, and tuffs from the Porrosatí and Carbonal Members, also act as aquitards, partially separating the Lower Barva from the Upper Barva.

2.2.1. Natural hydrogeochemical processes

The hydrolysis of Ca^{2+}-rich plagioclases and pyroxene in andesitic and andesitic-basaltic lavas is the primary process controlling the natural groundwater quality in the Barva aquifer along two chemically distinctive flow paths: the Barva north and south flow paths (Fig. 1d). These flow paths become enriched in NO_3^- and Cl^- as the pass through agricultural and urban areas lacking proper sewerage systems (Madrigal-Solís et al., 2022). The Na^+ and Mg^{2+} enriched Colima aquifers exhibit the typical hydrochemical evolution of mature groundwater with longer residence times, influenced by groundwater percolation through felsic volcanic rocks and weathering of aluminosilicates in andesites and trachyandesites along two chemically distinct flow paths: Upper Colima north and south flow paths (Fig. 1e). The Upper Colima aquifer is hydraulically connected to the underlying Mg^{2+}-enriched Lower Colima aquifer. Detailed hydrogeochemical processes of the Barva and Colima aquifers are described in Madrigal-Solís et al. (2022).

Seasonal variability in hydrogeochemical parameters was generally non-significant in most sampling sites ($n = 38$), in a study comprising 571 samples from the Barva and Colima aquifers (Madrigal-Solís et al., 2022). Significant seasonal differences ($p < 0.05$) were observed in only six sample sites from the Upper and Lower Barva aquifers, showing variations in one to four parameters, including NO_3^-. Sites within the Upper Barva aquifer exhibited higher temporal variability, with the Coefficient of Variation (CV) for NO_3^- exceeding 30 % in half of the cases, compared to the other three aquifers, where the CV remained below 30 % (Madrigal-Solís et al., 2022).

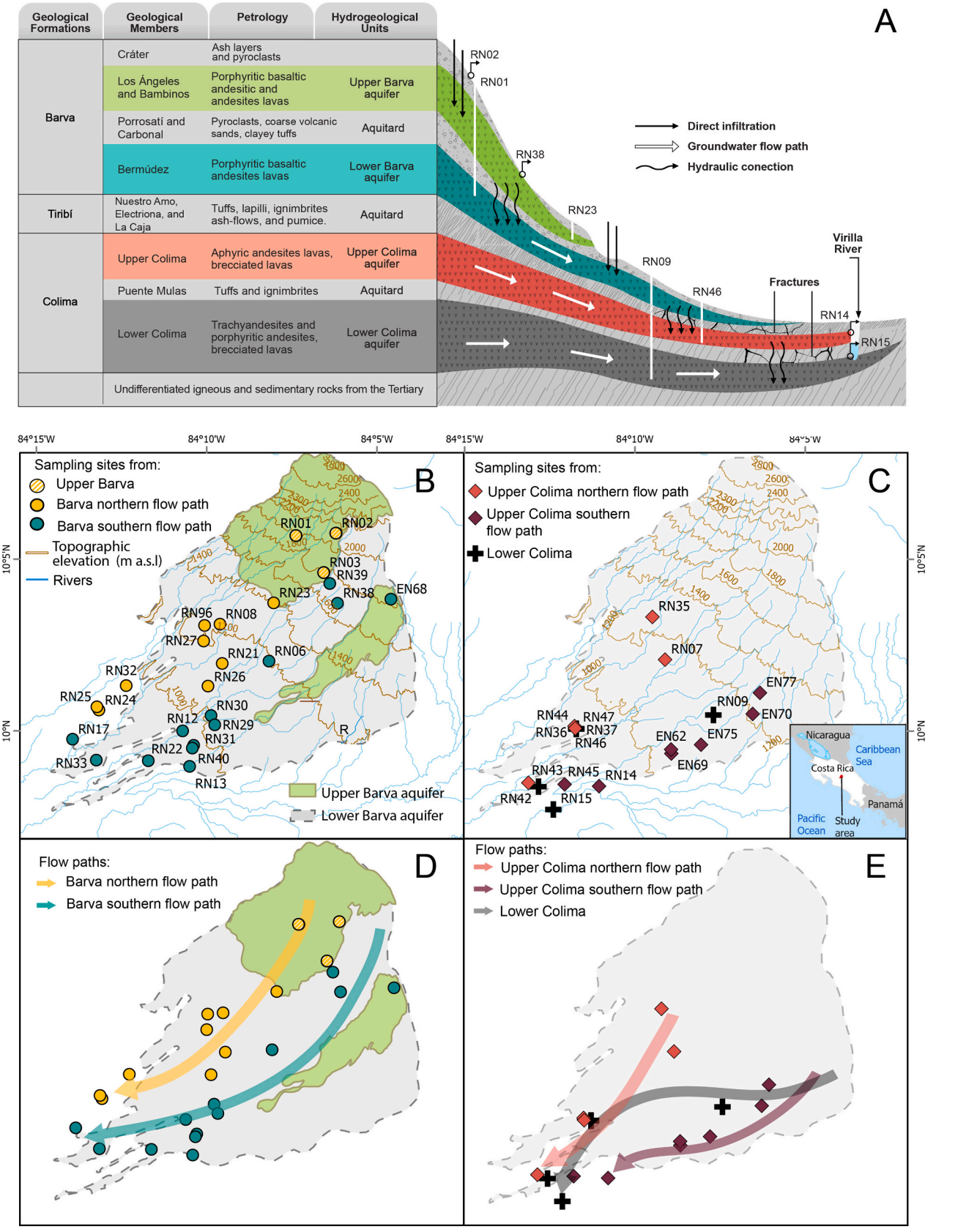

Fig. 1. (a) Simplified geology and hydrogeological cross-section for the Barva and Colima multi-aquifer system; groundwater sampling sites from (b) Barva aquifers and (c) Colima aquifers; groundwater flow paths in (d) Barva aquifer and (e) Colima aquifers, Central Valley, Costa Rica.

3. Materials and methods

3.1. Sampling and chemical and isotopic analyses

Between April 2015 and April 2022, 714 groundwater samples were collected quarterly from 43 sampling sites, including 11 springs and 32 pumping wells (Supplementary Table S2). These sites were distributed along preferential flow paths (Fig. 1b-e) and classified according to the primary aquifer withdrawn, prior studies, lithology information, and hydrochemical and discriminant analyses by Madrigal-Solís et al. (2022). Sampling occurred annually during the dry (April) and wet seasons (June, September, and December). In situ, electrical conductivity (EC in μS/cm), total dissolved solids (TDS), temperature (T), pH, and Eh were measured using portable instruments (HI98311 and HI98121, Hanna Instruments, USA), dissolved oxygen (DO) was measured with an HI 9147 sensor. Filtered samples (0.45 μm PTFE filter) were refrigerated at 4 °C and analyzed for major ions within a day (see Supplementary Text for details). Ion chromatography (Dionex Thermo Scientific ICS 5000) analyzed Ca^{2+}, Mg^{2+}, K^{+}, Na^{+}, Cl^{-}, nitrate (as NO_3^-), and sulfate (SO_4^{2-}), per method 4110 (American Public Health Association, 2012). Bicarbonate (HCO_3^-) was measured volumetrically using method 2310B (American Public Health Association, 2012). Samples with an ion balance error below 5 % were retained for further analysis.

Filtered samples for NO_2^-, NH_4^+, DOC, DIC, Mn_{total}, and Fe_{total} were collected in August and November 2021 (see Supplementary Text for details). NH_4^+ was analyzed by the 4500-NH_3-A method, and NO_2^- by the 4500 NO_2- B method using UV–Vis spectrophotometry (American Public Health Association, 2017). Fe_{total} and Mn_{total} were analyzed by ICP-MS spectrometry after microwave digestion. DOC and DIC were determined using a TOC analyzer (Aurora1030W, OI Analytical) and the Heated-Persulfate Oxidation Method 5310C (American Public Health Association, 2005).

$\delta^{15}N_{NO3}$ isotopes were assessed in March 2021 ($n = 14$) and August 2021 ($n = 16$). Sites were selected based on spatial representativeness and a historical mean NO_3^- concentration > 5 mg/L (Madrigal-Solís et al., 2022), prioritizing NO_3^- contaminated sites and the reduction of analytical uncertainties. Samples were filtered through a 0.45 μm filter and frozen until analysis. The analysis was performed in duplicate at the Environmental Isotope Laboratory of the University of Waterloo using an Isoprime Trace Gas Continuous Flow mass spectrometer (GV Instruments Ltd., Manchester, UK), with a precision of $2\sigma = 1.0$ ‰ VSMOW/0.5 ‰ Air-N2. NO_3^- was converted to NO_2^- through cadmium catalysis and then to N_2O. Calibration involved standards USGS34, USGS35, in-house EGC17, and check standards EGC1 and IAEA NO-3 during each sample run, with linearity checks using 100 ppm N_2O in helium mixtures with known isotopic compositions.

3.2. Land-use and land-cover (LULC), point pollution sources, and statistical analyses

LULC analysis for 2021 was conducted using 0.5 m high-resolution Maxar satellite imagery, categorizing land into forest, agricultural fields, pastures, and urban areas with ArcGIS Pro 2.5.0. The study area was divided into upper (1600–2800 m a.s.l.), middle (1100–1600 m a.s.l.), and lower zones (850–1100 m a.s.l.). Data on dairy, pig, and poultry farms were collected from the National Animal Health Service (SENASA) to identify potential NO_3^- and OM pollution sources in November 2021. Population density and wastewater discharge were estimated by the altitudinal sector using district-level population projections for 2022 (INEC, 2018) and a per capita wastewater generation of 0.2 m^3/day (ICAA et al., 2016).

Hydrochemical data analysis included Shapiro-Wilk normality tests and correlation coefficients using SPSS Statistics (IBM Corp, 2021). The Mann-Whitney *U* test, PCA, and HCA with Ward's linkage and squared Euclidean distance were performed using XLSTAT (Addinsoft, 2023). Before the PCA and HCA, data sets were log-transformed (Log_{10}) and z-score standardized. Two PCAs were conducted, with and without $\delta^{15}N_{NO3}$ isotopes, to evaluate the necessity of isotopic information in the identification of groundwater quality factors. Two HCAs were also performed to group study sites based on contamination indicators, with and without $\delta^{15}N_{NO3}$ isotopes, to validate contamination sources and assess isotopic effectiveness. Selection criteria for the PCAs included variables with factor loadings >0.65, eigenvalues >1 in the first two PCs, Bartlett Chi-square tests ($p < 0.001$), and KMO results >0.75 (Huang et al., 2023; Meghdadi and Javar, 2018; Torres-Martínez et al., 2021). These variables were also used in HCA analyses. Statistical correlations and differences were based on a significance level of $p < 0.05$.

4. Results

4.1. LULC patterns

The regional LULC within the Barva aquifer revealed that nearly 30 % of the total area is covered by forest, 30 % by agricultural lands, 30 % by urban areas, and 10 % by pasture for cattle grazing (Fig. 2a). LULC shows an altitudinal distribution: at higher elevations, 66 % is forest and 23 % is pasture for low-density cattle grazing. The mid-altitude zone has an Agriculture/Urban LULC type, with 56 % of agricultural fields (mainly coffee farms) and 20 % of urban areas. In the lower zone, the Urban LULC type is covered by 63 % of urban areas and 16 % of agricultural fields (Fig. 2b). Population density rises from 375 people/km^2 in Forest/Grassland areas to 1800 people/km^2 in Agricultural zones, peaking at 4840 people/km^2 in urban areas. With a per capita wastewater generation rate of 0.2 m^3/day (ICAA et al., 2016) and a total population of 473,491 projected for 2022 (INEC, 2018), the study area produces an estimated 94,700 m^3/day of wastewater. Of this, 6 % is generated in the Forest/Grassland, 16 % in Agricultural/Urban zones, and 78 % in urban areas.

4.2. General physical, chemical, and isotopic parameters

The statistical summary corresponding to the physical parameters, major ions, and NO_3^- for 714 samples from the four studied aquifers and flow paths is shown in Table 1 and Supplementary Table S3. According to the Piper diagram (Supplementary Fig. S2), samples from the Barva aquifer and Upper Colima south flow path are classified as non-dominant-HCO_3 facies (with a higher Ca^{2+} content), gradually transitioning to HCO_3-Cl type along the flow path. Samples from the Upper Colima north flow path and Lower Colima aquifer are Mg-HCO_3 type, transitioning towards HCO_3-Cl-SO_4 non-dominant type. Comprehensive hydrogeochemical characterization of the Barva and Colima multi-aquifer system, including comparisons between aquifers, flow paths, and seasons is detailed in Madrigal-Solís et al. (2022).

4.3. Barva aquifer pollution patterns

In the high-altitude zone, the Upper Barva aquifer has the lowest mean NO_3^- values (Table 1). In the Lower Barva aquifer, results indicate that 52 % of the 474 samples exceeded the nitrate (as NO_3^-) Alert Value (AV) of 25 mg/L, and 12 samples exceeded the Maximum Concentration Level (MCL) of 50 mg/L, according to the Regulation for Drinking Water Quality of Costa Rica (2015).

The evaluation of the spatial hydrochemical evolution and the impact of certain contamination processes requires a flow path-centered approach. Due to significant differences in most hydrochemical parameters between the north and south flow paths (Madrigal-Solís et al., 2022), these are evaluated separately in the present research to assess contamination dynamics (Fig. S1). As natural processes may not fully account for the chemical variations between flow paths (Madrigal-Solís et al., 2022), it is hypothesized that these differences are the result of distinct anthropogenic pressures.

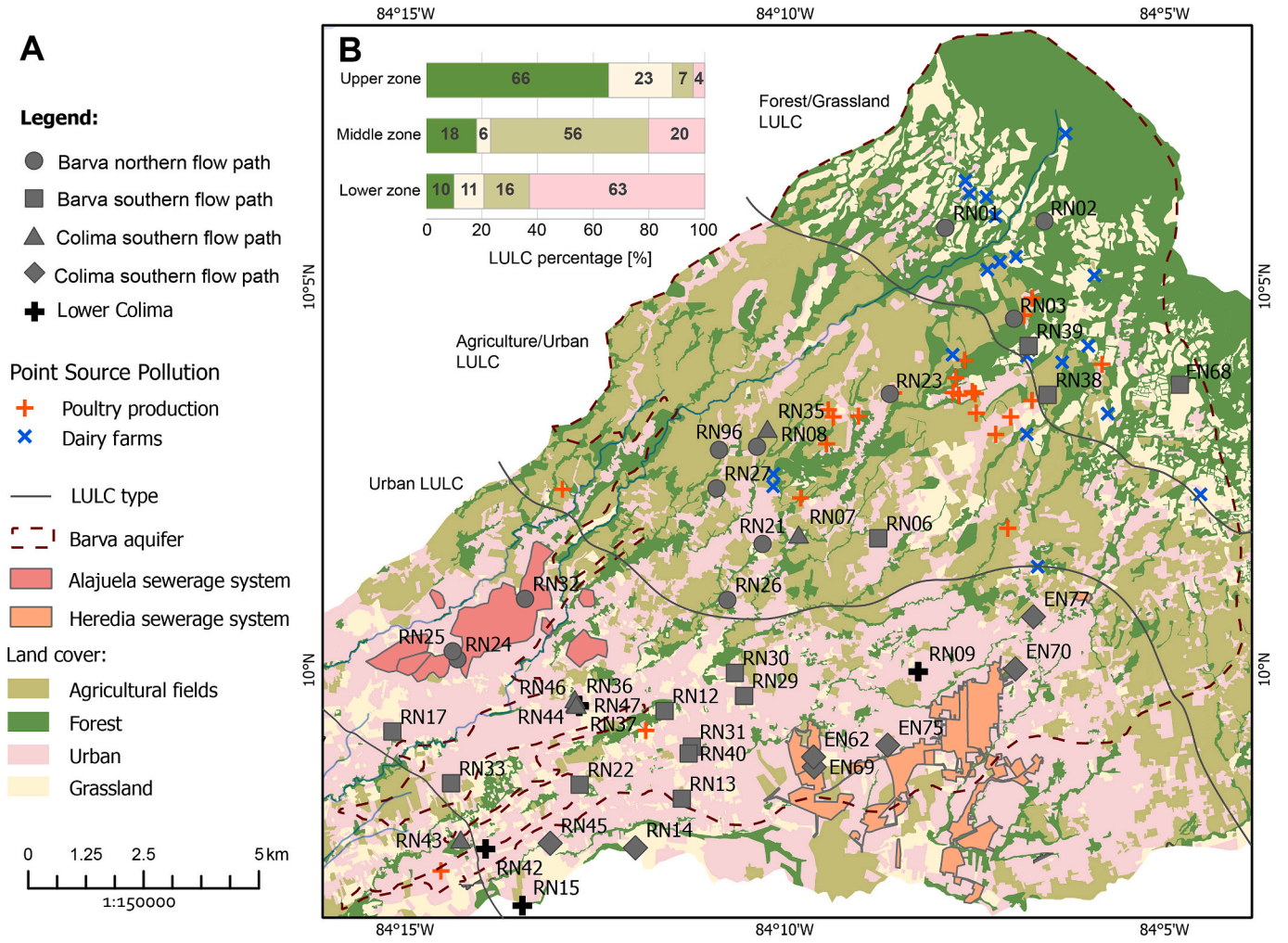

Fig. 2. Anthropogenic activities and sampling points in the study area, including (a) land cover, sewerage systems, poultry and dairy farms, and (b) percentages of land cover in the upper, middle, and lower zones in the study area, Central Valley, Costa Rica.

4.3.1. Hydrochemical evolution along preferential flow paths in Barva aquifer

The median NO_3^- concentration in the north path (35 mg/L) is higher than in the south path (22.5 mg/L), with maximum values of 110.7 mg/L in the north and 52.1 mg/L in the south (Table 1, Fig. 3b). The north path also shows higher mean NO_2^- and lower mean K^+, Na^+, HCO_3^-, SO_4^{2-}, and DOC values compared to the south path (Table 1). NO_3^- and Cl^- correlate more strongly with distance when Upper Barva samples are merged into the Lower Barva north path (Fig. 3a-c), as Upper Barva partially recharges the Barva aquifer (BGS/SENARA, 1988; Madrigal-Solís et al., 2022). In the south flow path, DOC correlations with distance are stronger, with DOC increasing significantly near the discharge zone (Fig. 3d-e). Both paths show a strong correlation of DIC with distance (Fig. 3f), decreasing NO_2^- and DO concentrations (Fig. 4a-b), and spatially stable Eh, Fe_{total}, Mn_{total}, and NH_4^+ values (Supplementary Fig. S3a-d). DIC increases with increasing NO_3^- (Fig. 4c), but no correlation is found between NH_4^+ and NO_3^- (Supplementary Fig. S3e). An excess of HCO_3^- is observed with respect to the hydrolysis of dominant Ca^{2+}–rich plagioclase, especially along the south flow path (Fig. 4d-e). A stronger correlation between Na^+ and Cl^- was found in the south path, aligning with a 1:1 equiline, while the north path shows a higher Cl^- to NO_3^- ratio (Fig. 4f).

4.3.2. Hydrochemical and isotopic profiles across the LULC patterns in Barva aquifer

An increase in $\delta^{15}N_{NO3}$ values (r = 0.79) was observed as groundwater traveled from agricultural to urban areas (Fig. 5a). Locations within the Agriculture/Urban LULC region had DOC values <1.6 mg/L and $\delta^{15}N_{NO3}$ values from +2.6 to +9.5 ‰, while Urban LULC sites showed values ranging from +7.2 to +11 ‰ (Fig. 5a, b). There was a linear relationship between $\ln(NO_3^-)$ and $\delta^{15}N_{NO3}$ (r = 0.73, Fig. 5c).

Two PCAs and HCAs analyzed the impact of LULC on NO_3^- contents, utilizing variables with significant loadings and correlations (Table 2a-b). Including $\delta^{15}N_{NO3}$ isotopes, PCA explained 82.5 % of the total variance in the first PCs. PCA and HCA identified two clusters: an Agricultural/Urban (C1), linked to Mn_{total}, Fe_{total}, NO_2^-, and an Urban cluster (C2) strongly related to higher $\delta^{15}N_{NO3}$, DOC, Cl^-, K^+, and Na^+ (Fig. 6a-b). Excluding $\delta^{15}N_{NO3}$, PCA still captured 77.6 % of the total variance and, along with the HCA (Fig. 6c-d), grouped sites into Forest/Grassland (C1), Agricultural/Urban (C2), associated with NO_2^- and Fe_{total}, and Urban (C3), related to DOC, HCO_3^-, NO_3^-, Cl^-, Ca^{2+}, K^+, and Na^+. All clusters, with and without the isotopic information, coincide with the LULC pattern in each sample location.

By classifying all samples from 2015 to 2022 according to the HCA clusters (Fig. 6e), higher K^+ values were observed in the Urban clusters (C3 and C4) compared to other clusters (p-value <0.001). Median NO_3^- values were lower in Forest/Grassland LULC (1.8 mg/L) and increased to 27.8 and 27.9 mg/L in Agricultural/Urban and Urban areas (Fig. 3b, Table 3) with no significant difference between the latter two (p-value = 0.289). Spearman correlation coefficients showed a higher positive correlation between NO_3^- and Cl^- in the Agricultural/urban LULC (r = 0.81) compared to Urban LULC (r = 0.73) (Supplementary Table S5).

Table 1
Statistical information for physical and chemical parameters and test of normality in samples from Barva and Colima aquifers and flow paths, in Central Valley, Costa Rica.

Parameter	Aquifer flow/ path	n	Min	Max	Median	Mean	SD	Parameter	Aquifer flow/ path	n	Min	Max	Median	**Mean**	**SD**
Eh	**UB**	***75***	0.22	0.68	0.40	0.41	0.29	**HCO_3^-**	**UB**	***75***	19.2	78.6	34.4	36.8	11.0
[V]	**B1**	***150***	0.26	1.00	0.41	0.42	0.32	**[mg/L]**	**B1**	***150***	31.0	144.2	68.8	74.7	25.4
	B2	***249***	0.27	0.92	0.43	0.45	0.30		**B2**	***249***	42.5	165.3	92.7	94.0	21.3
	UC1	***100***	0.21	0.68	0.42	0.42	0.28		**UC1**	***100***	56.5	123.3	88.0	88.1	18.0
	UC2	***49***	0.37	0.58	0.46	0.47	0.27		**UC2**	***49***	66.4	138.5	109.2	110.3	16.4
	LC	***91***	0.26	0.83	0.41	0.42	0.30		**LC**	***91***	73.7	163.9	114.4	116.4	16.0
DO	**UB**	***75***	1.6	9.1	7.3	6.7	1.8	**Mg^{2+}**	**UB**	***75***	1.0	6.4	3.4	3.9	1.7
[mg/L]	**B1**	***150***	2.5	9.6	5.6	5.7	1.6	**[mg/L]**	**B1**	***150***	1.3	17.1	8.4	8.4	2.7
	B2	***249***	2.0	9.5	6.0	5.7	1.5		**B2**	***249***	3.3	15.2	8.7	8.5	2.1
	UC1	***100***	3.4	10.1	6.0	5.8	1.4		**UC1**	***100***	5.0	14.8	10.5	11.3	2.6
	UC2	***49***	3.5	9.1	7.2	6.8	1.6		**UC2**	***49***	5.0	12.4	10.0	10.6	1.8
	LC	***91***	3.1	9.6	6.6	6.6	1.5		**LC**	***91***	6.6	18.4	12.7	12.8	2.9
TDS	**UB**	***75***	11.0	199.0	54.0	64.2	39.6	**SO_4^{2-}**	**UB**	***75***	2.6	32.9	11.9	13.2	7.4
[ppm]	**B1**	***150***	16.0	328.0	115.0	125.0	50.9	**[mg/L]**	**B1**	***150***	0.8	11.4	3.9	3.6	2.3
	B2	***249***	32.0	374.0	115.0	124.8	51.0		**B2**	***249***	1.1	18.5	7.0	5.3	4.2
	UC1	***100***	42.0	260.0	113.0	117.0	38.0		**UC1**	***100***	0.7	28.1	19.0	23.1	9.3
	UC2	***49***	34.0	235.0	129.6	133.4	39.5		**UC2**	***49***	1.8	9.7	6.7	7.2	1.9
	LC	***91***	49.0	361.0	139.5	155.1	56.7		**LC**	***91***	5.7	38.4	21.6	26.1	11.5
pH	**UB**	***75***	5.2	7.8	6.5	6.5	0.7	**DOC**	**UB**	***10***	0.03	1.71	0.65	0.80	0.85
	B1	***150***	5.5	7.3	6.3	6.4	0.4	**[mg/L]**	**B1**	***14***	0.95	2.29	1.59	1.60	0.51
	B2	***249***	5.5	7.7	6.4	6.5	0.4		**B2**	***24***	0.15	10.29	1.55	3.33	3.59
	UC1	***100***	5.6	7.5	6.7	6.8	0.4		**UC1**	***12***	0.22	11.39	1.30	2.71	4.28
	UC2	***49***	5.8	7.5	6.6	6.6	0.4		**UC2**	***12***	0.26	5.86	2.04	2.75	2.10
	LC	***91***	5.8	7.9	6.9	6.9	0.4		**LC**	***10***	1.43	3.70	1.53	2.07	0.97
T	**UB**	***75***	10.4	26.2	18.6	18.5	2.5	**DIC**	**UB**	***10***	1.47	10.29	8.14	6.63	4.60
[°C]	**B1**	***150***	16.4	25.9	22.6	22.9	2.2	**[mg/L]**	**B1**	***14***	11.03	22.04	15.97	16.52	4.29
	B2	***249***	14.4	25.5	22.5	22.2	3.5		**B2**	***24***	2.06	26.39	13.19	12.16	6.97
	UC1	***100***	20.2	27.5	23.0	22.8	1.4		**UC1**	***12***	0.03	14.38	13.36	11.08	5.49
	UC2	***49***	20.2	25.8	22.0	21.9	1.0		**UC2**	***12***	4.26	19.45	15.95	13.29	7.12
	LC	***91***	17.1	24.8	22.4	22.3	1.1		**LC**	***10***	6.39	17.46	16.48	14.33	4.56
EC	**UB**	***75***	33.0	385.0	131.5	109.5	75.8	**NH_4^+**	**UB**	***10***	26.3	38.9	30.1	31.8	6.4
[µS/cm]	**B1**	***150***	70.0	540.0	242.3	231.5	91.0	**[µg/L]**	**B1**	***14***	24.0	39.1	26.5	28.8	5.3
	B2	***249***	69.0	720.0	236.2	222.5	95.5		**B2**	***24***	19.8	35.6	25.6	26.8	5.2
	UC1	***100***	60.0	667.0	227.1	219.5	83.6		**UC1**	***12***	22.2	48.0	25.6	29.2	9.6
	UC2	***49***	74.0	470.0	231.5	236.0	70.4		**UC2**	***12***	16.9	57.8	22.2	28.7	16.6
	LC	***91***	160.0	728.0	296.0	263.5	108.4		**LC**	***10***	26.2	38.9	28.2	31.1	5.9
NO_3^-	**UB**	***75***	0.8	15.3	2.9	5.1	4.3	**NO_2^-**	**UB**	***10***	3.6	15.0	14.5	11.0	6.4
[mg/L]	**B1**	***150***	0.3	110.7	35.0	34.4	16.4	**[µg/L]**	**B1**	***14***	3.4	38.2	12.0	13.3	12.4
	B2	***249***	0.9	52.1	22.5	22.5	9.7		**B2**	***24***	3.0	27.6	3.9	8.2	7.9
	UC1	***100***	2.6	20.9	9.5	9.1	4.7		**UC1**	***12***	3.3	18.7	10.4	10.3	5.2
	UC2	***49***	10.8	58.5	20.1	20.2	3.5		**UC2**	***12***	3.6	6.6	4.4	4.7	1.1
	LC	***91***	1.7	14.5	5.2	6.0	3.3		**LC**	***10***	3.0	13.2	7.0	7.3	3.8
Cl^-	**UB**	***75***	0.9	7.0	1.9	2.4	1.4	**Fe_{total}**	**UB**	***10***	3.3	6.1	4.7	4.3	2.0
[mg/L]	**B1**	***150***	1.1	24.6	9.0	10.3	6.2	**[µg/L]**	**B1**	***14***	18.5	136.0	51.0	24.7	56.9
	B2	***249***	1.1	22.1	6.4	9.2	3.6		**B2**	***24***	10.9	114.0	34.9	16.0	36.3
	UC1	***100***	2.0	17.7	10.0	9.4	4.0		**UC1**	***12***	13.8	40.7	23.7	20.7	9.8
	UC2	***49***	3.6	12.4	9.8	9.5	2.2		**UC2**	***12***	6.2	121.0	28.7	10.7	45.4
	LC	***91***	5.6	33.0	17.1	17.3	7.2		**LC**	***10***	14.9	23.9	19.5	19.7	4.5
Ca^{2+}	**UB**	***75***	4.5	15.5	8.1	8.5	2.9	**Mntotal**	**UB**	***10***	0.2	10.1	3.6	0.4	5.7
[mg/L]	**B1**	***150***	4.6	38.8	20.2	20.6	6.4	**[µg/L]**	**B1**	***14***	8.6	18.9	12.4	9.9	4.6
	B2	***249***	6.7	33.8	20.9	20.6	5.8		**B2**	***24***	1.2	19.0	7.5	7.0	4.2
	UC1	***100***	11.7	20.2	15.6	15.8	2.1		**UC1**	***12***	7.5	13.8	9.4	8.6	2.3
	UC2	***49***	13.8	26.0	21.7	21.1	2.8		**UC2**	***12***	0.3	10.8	3.5	0.5	4.8
	LC	***91***	8.7	26.3	16.3	16.3	2.1		**LC**	***10***	6.0	10.5	8.8	9.0	1.8
Na^+	**UB**	***75***	2.7	9.2	4.3	4.4	1.1	**$\delta^{15}N_{NO3}$**	**B1**	***11***	2.6	11.0	8.4	7.2	3.1
[mg/L]	**B1**	***150***	3.6	11.6	5.9	6.2	1.5	**[‰]**	**B2**	***10***	4.7	10.3	7.2	7.3	1.9
	B2	***249***	3.5	13.7	7.0	7.4	2.2		**UC1**	***4***	3.8	12.8	7.0	7.6	4.2
	UC1	***100***	3.9	19.0	10.5	9.6	4.0		**UC2**	***2***	8.3	8.6	8.4	8.4	0.2
	UC2	***49***	5.7	12.2	10.4	9.8	1.7		**LC**	***2***	6.6	7.3	6.9	6.9	0.5
	LC	***91***	7.2	32.4	14.8	18.0	6.6								
K^+	**UB**	***75***	1.5	3.4	2.2	2.2	0.4								
[mg/L]	**B1**	***150***	1.0	5.6	2.3	2.8	1.2								
	B2	***249***	1.2	6.6	3.2	3.3	0.8								
	UC1	***100***	1.3	6.2	4.2	3.7	1.4								
	UC2	***49***	3.5	5.8	4.5	4.4	0.4								
	LC	***91***	2.4	12.7	5.8	6.9	2.5								

UB: Upper Barva; B1: Barva northern flow path; B2: Barva southern flow path; UC1: Upper Colima northern flow path; UC2: Upper Colima southern flow path; LC: Lower Colima.

EC: electrical conductivity; T: temperature; DO: dissolved oxygen; Eh: redox potential; TDS: total dissolved solids; DIC: Dissolved Inorganic Carbon, DOC: Dissolved Organic Carbon; S-W: Shapiro-Wilk test.

Limits of detection (LD) and quantification (LQ): NO_3^- (0.11 and 0.35 mg/L), Cl^- (0.06 and 0.19 mg/L), NH_4^+ (0.1 and 14 µg/L), NO_2^- (3.6 and 10.3 µg/L), Fe_{total} (3.0 and 3.4 µg/L), Mn_{total} (0.24 and 0.69 µg/L), DOC and DIC (0.05 and 0.03 mg C/L); HCO_3^- (LQ = 1.3 mg/L), SO_4^{2-} (0.081 and 0.24 mg/L), Na^+ (0.16 and 0.48 mg/L), Mg^{2+} (0.19 and 0.57 mg/L), K^+ (0.052 and 0.16 mg/L); Ca^{+2} (0.28 and 0.84 mg/L).

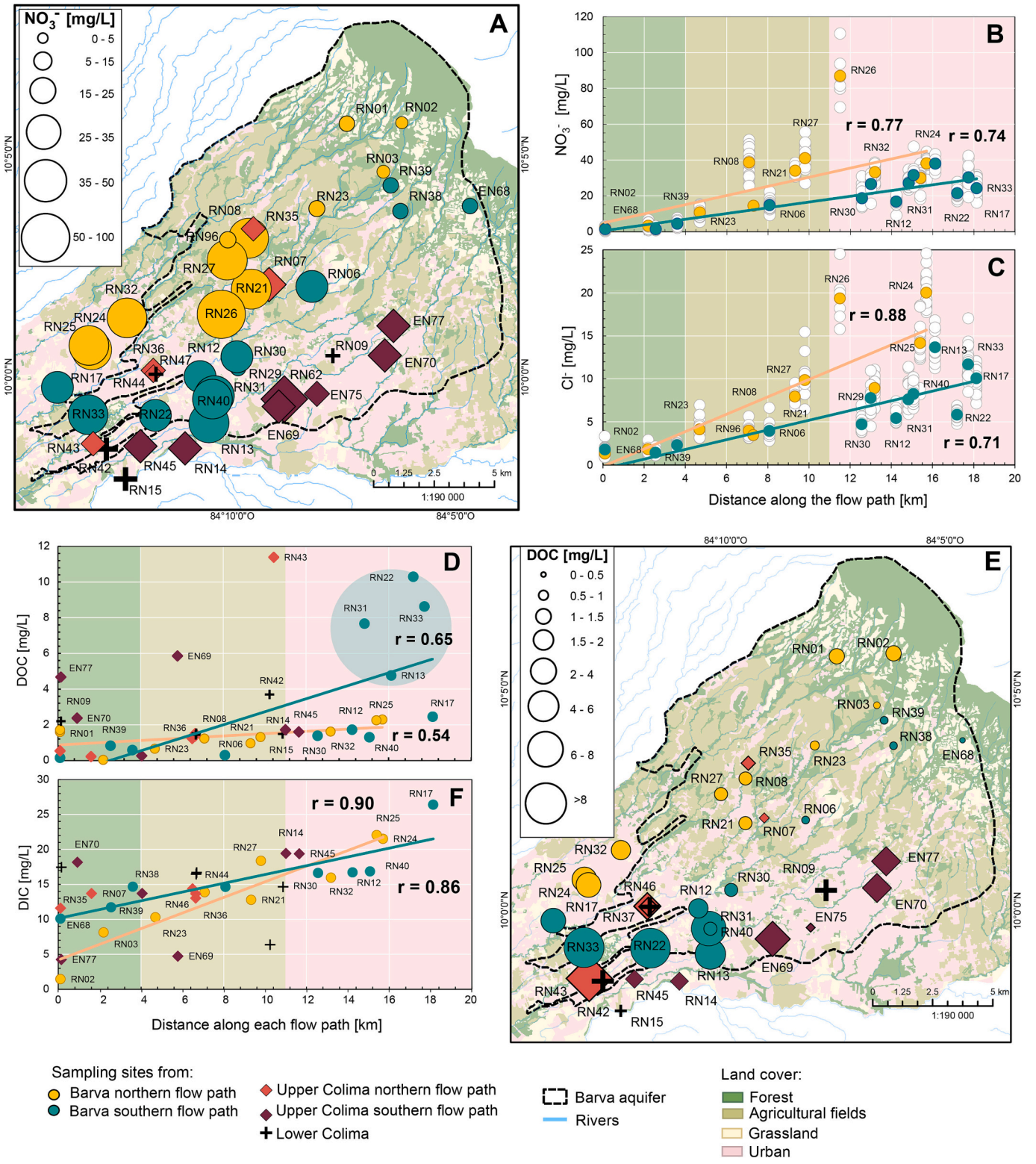

Fig. 3. Spatial distribution of (a) median nitrate concentrations; distance along each flow path vs. (b) nitrate, (c) chloride, and (d) dissolved organic carbon (DOC); (e) spatial distribution of DOC; and (f) distance along each flow path vs. dissolved inorganic carbon (DIC) for groundwater in Barva and Colima multilayer aquifer system, Central Valley, Costa Rica.

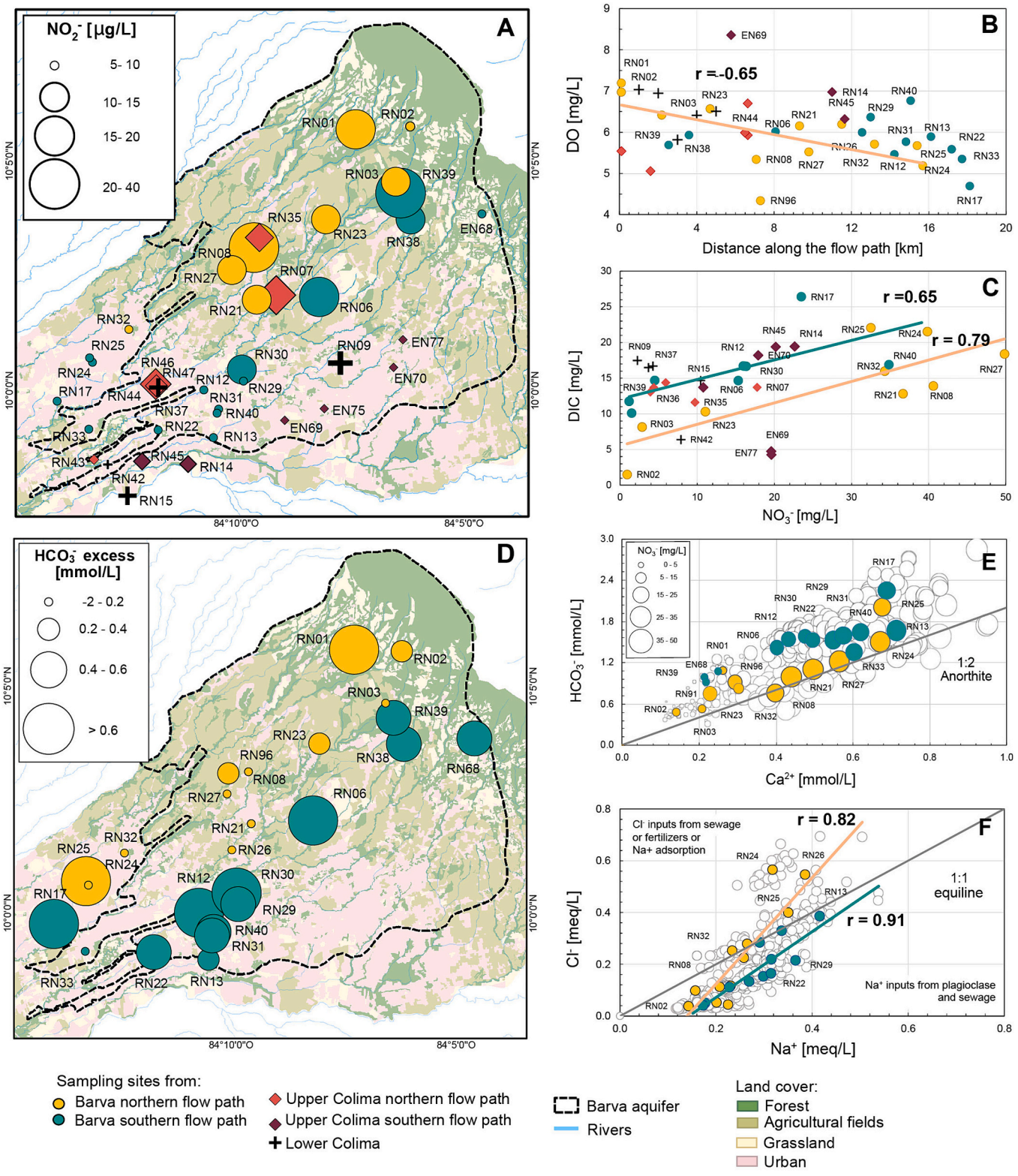

Fig. 4. Spatial distribution of (a) median nitrite concentrations; (b) distance along each flow path vs dissolved oxygen (DO); (c) nitrate vs dissolved inorganic carbon (DIC); (d) spatial distribution of bicarbonate excess with respect to calcium; (e) calcium vs bicarbonate; and (f) sodium vs chloride for groundwater in Barva and Colima multilayered system, Central Valley, Costa Rica.

4.4. Upper and Lower Colima aquifers

Among the 240 samples collected from deeper Colima aquifers, eight samples exceeded the nationally defined Alert Value (AV) of 25 mg/L for NO_3^- and three exceeded the MCL.

4.4.1. Spatial variability and correlations along Colima flow paths

Significant differences were observed between the Upper Colima flow paths by Madrigal-Solís et al. (2022). Thus, the investigation into the Upper Colima flow paths (Fig. S1) highlighted distinct contamination processes, particularly in the south path. The median NO_3^-

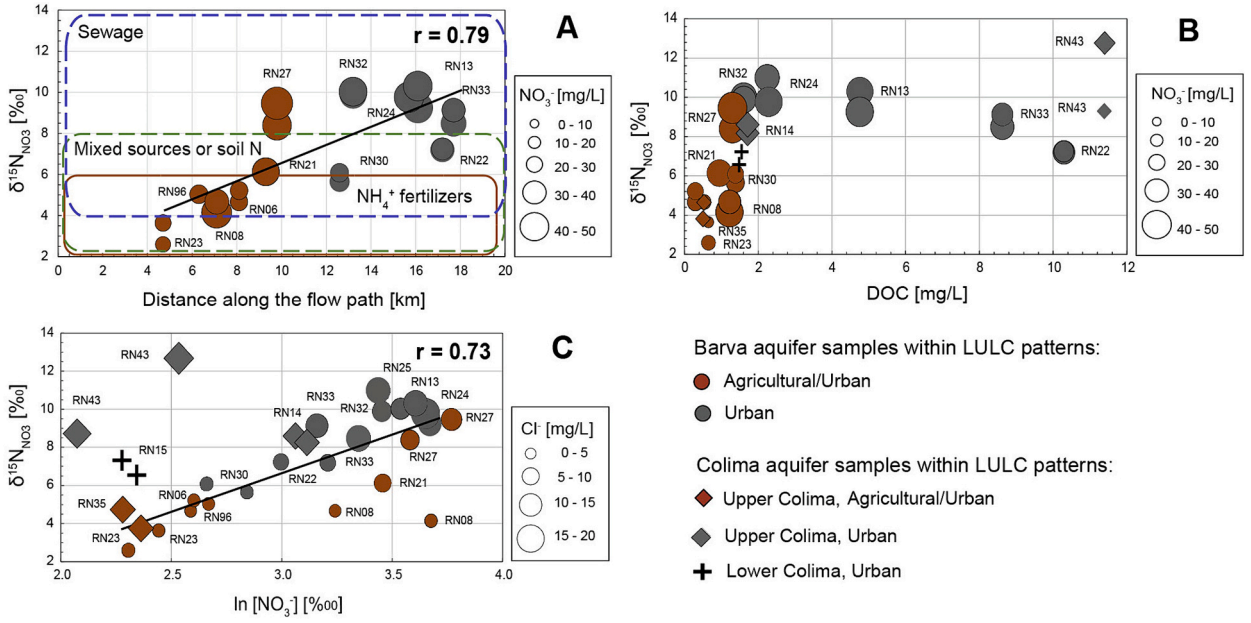

Fig. 5. (a) Distance along the flow path vs δ15NNO3, (b) ln(NO3-) vs δ15NNO3, and (c) dissolved organic carbon vs $\delta^{15}N_{NO3}$ for groundwater in Barva and Colima multilayered aquifer system, Central Valley, Costa Rica.

Table 2
Factor loadings, eigenvalues and cumulative variance explained for the PCA in (a) Barva aquifer, and (b) Barva and Colima aquifers, in Central Valley, Costa Rica.

(a) Barva and Colima aquifers, including δ15NNO3			(b) Barva aquifer samples, including only hydrochemical parameters		
Variable	**F1**	**F2**	**Variable**	**F1**	**F2**
DOC	**0.910**	−0.296	HCO3-	**0.899**	0.009
NO_2^-	**−0.909**	0.116	DOC	**0.746**	−0.392
Cl^-	**0.823**	0.370	NO_2^-	−0.557	**0.619**
$\delta^{15}N_{NO3}$	**0.848**	−0.005	NO_3^-	**0.686**	0.460
K^+	**0.726**	0.518	Cl^-	**0.915**	0.112
Fe	**−0.877**	0.267	K^+	**0.743**	−0.081
Mn	**−0.818**	0.420	Fe_{Total}	−0.236	**0.771**
Na^+	**0.850**	0.325	Ca^{+2}	**0.938**	0.075
Eigenvalue	5.7	0.9	Na^+	**0.950**	0.061
Total variance (%)	71.7	10.7	Eigenvalue	6.3	1.5
Cumulative variance (%)	71.7	82.5	Total variance (%)	63.0	14.5
			Cumulative variance (%)	63.0	77.6

concentration in the Upper Colima south path was 20.2 mg/L, similar to that in the Barva south path, twice as high as in the Upper Colima north path, and four times higher than in the Lower Colima aquifer (Table 1). The south paths of both Upper Colima and Barva had the highest DOC and the lowest mean concentrations of NO_2^-, Fe_{total}, and $Mn_{total.}$, compared to the Upper Colima north path and Lower Colima (Table 1). Correlation analysis shows mostly non-significant relationships between chemical parameters and distance along the flow paths for the Upper and Lower Colima aquifers (Supplementary Table S4). Near agricultural zones, the Upper Colima north path had higher concentrations of NO_3^- and NO_2^-, with increased DOC levels in the lower zone (Figs. 3a, e, and 4a). The south path exhibits higher concentrations of NO_3^- and DOC near urban centers like Heredia and Alajuela, (Figs. 3a, e, and 4a). Both Upper and Lower Colima aquifers showed oxidizing conditions, with stable DO and Eh values and low levels of Fe_{total}, Mn_{total}, NO_2^-, and NH_4^+ in most sampling sites (Table 1, Fig. 4b, Fig. S2).

4.4.2. Multivariate statistical analyses, DOC, and $\delta^{15}N_{NO3}$ values across LULC patterns in Colima aquifers

Samples from Agricultural/Urban areas showed DOC levels < 1 mg/L and $\delta^{15}N_{NO3}$ values near +4 ‰, while those within the Urban LULC exhibited DOC values > 1 mg/L and $\delta^{15}N_{NO3}$ values ranging from +8.4 to +12.8 ‰ (Fig. 5b). These $\delta^{15}N_{NO3}$ fall within the expected range for sources such as ammoniacal fertilizers, soil nitrogen, and sewage (Kendall et al., 2007; Xue et al., 2009). In contrast to the Barva aquifer, samples in the Colima aquifers did not show a clear linear relationship between ln(NO_3^-) vs. $\delta^{15}N_{NO3}$ (Fig. 5c). In the PCA including $\delta^{15}N_{NO3}$ values, the four samples from the Colima aquifers were grouped into two subgroups alongside Barva aquifer samples (Fig. 6a). Colima samples in the urban areas clustered in the positive segment of Factor 1 (F1), closely associated with DOC, $\delta^{15}N_{NO3}$, Cl^- and Na^+, while the RN35 sample near agricultural fields fell into the negative segment, close to Fe_{total}, Mn_{total}, NO_2^-, and opposite to DOC. This pattern aligned with the Barva aquifer samples in the Agricultural/Urban LULC. In the HCA of Fig. 7, which included all Barva and Colima samples and excluded NO_3^- isotopes, the 17 samples from the Colima aquifer with hydrochemical information were classified into three clusters: C2, characterized by low NO_3^- and DOC in urban areas; C3, showing moderate NO_3^- and low DOC in agricultural/urban areas, and C4 exhibiting moderate to high NO_3^-concentrations and moderate to high DOC levels in urban areas.

5. Discussion

5.1. Contamination in Barva aquifer

The extensive hydrochemical analysis reveals significant spatial variations in NO_3^- and DOC across different LULC patterns, especially in the Barva aquifer. Agricultural/urban areas in the mid-altitude zone, particularly coffee farms, and urban land use at lower elevations contributed to similar median NO_3^- contents (Table 3, Figs. 2 and 3a). The widespread NO_3^- contamination in the Barva aquifer, indicated by 52 % of the 474 samples exceeding the Alert Value of 25 mg/L and 12 samples exceeding the 50 mg/L NO_3^- of MCL (with a maximum value of 110.7 mg/L in the Agricultural/Urban LULC sector, Fig. 3b), poses significant risks to water quality and public health. Historically, from 1988 to 2011, NO_3^- concentrations rarely exceeded the Alert Value and never

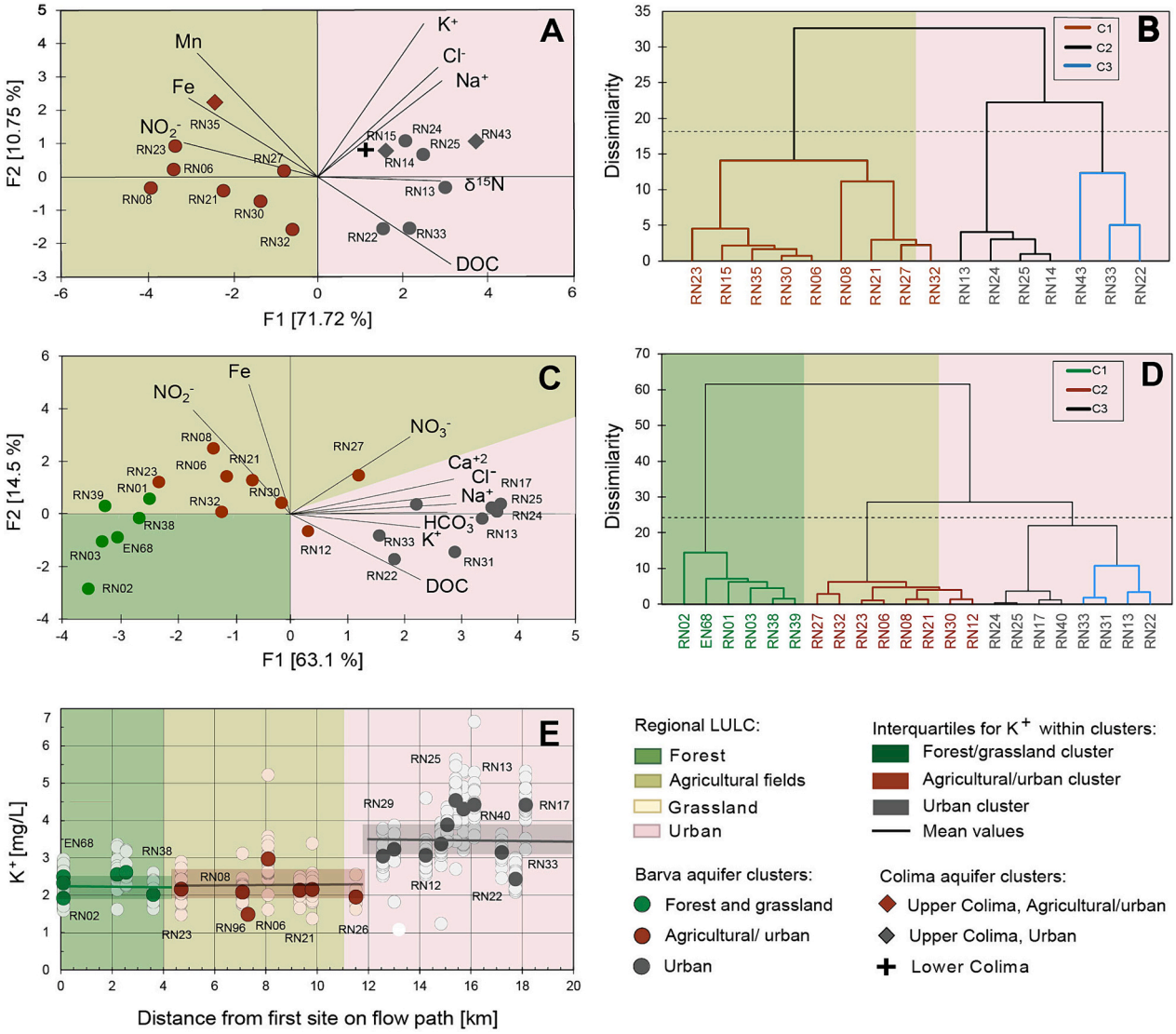

Fig. 6. Sampling sites classified by clusters: (a) Principal components analyses (PCA) and (b) Hierarchical Cluster Analysis (HCA), including $\delta^{15}N_{NO3}$; (c) PCA and (d) HCA, excluding $\delta^{15}N_{NO3}$; (e) distance along the flow path vs potassium for the multilayered aquifer system, Central Valley, Costa Rica.

surpassed the MCL (Reynolds-Vargas et al., 2006; Madrigal-Solís et al., 2017, 2019). Moreover, Sánchez-Gutiérrez et al. (2023) found that only 10 % of samples exceeded the 25 mg/L. The observed differences in concentrations can be attributed to the increased number of sampling sites (n = 43) and samples collected (n = 714) in the current study, including 474 samples from the Barva aquifer.

5.2. *Nitrification processes controlling NO_3^- concentrations in Barva aquifer*

In the Barva aquifer, positive correlations between DIC and NO_3^- support the efficient mineralization of DOC into DIC and further nitrification, particularly in aerobic conditions (Fig. 4c) (Gao et al., 2021; Hosono et al., 2015). Surprisingly, despite the positive correlation of NO_3^- with distance traveled along the Barva north (r = 0.77) and south (r = 0.74) flow paths (Fig. 3b), no significant differences were found between the middle and lower sections of the study area (Table 3). This similarity in NO_3^- concentrations is likely due to dilution from substantial recharge during extensive tropical rainy seasons, from May to mid-December (Magaña et al., 1999; Maldonado et al., 2013), rather than a widespread NO_3- reduction process.

In anoxic or subanoxic conditions, heterotrophic denitrification can occur, where anaerobic bacteria use DOC and NO_3^- with Fe/Mn oxides as electron acceptors, resulting in increased NH_4^+, NO_2^-, Fe_{total}, or Mn_{total} concentrations, and decreased NO_3^- (Gao et al., 2021). However, stable oxidizing conditions, favorable DO levels, increasing NO_3^-, and low levels of NH_4^+, NO_2^-, Fe_{total}, or Mn_{total} (Supplementary Fig. S3) suggest that heterotrophic denitrification is not occurring. The NO_3^- plot (Fig. 5c) also contradicts the expected trend for denitrification (Kendall, 1998). Additionally, there was no evidence of dissimilatory nitrate reduction to ammonium (DNRA), given the low NH_4^+ and rising NO_3^- levels (Rivett et al., 2008; Rütting et al., 2011; Kraft et al., 2014).

In agricultural areas, NH_4^+ might primarily originate from urea and ammoniacal fertilizers (NH_4NO_3), commonly used in coffee plantations in the Central Valley (ICAFE, 2020). In urban areas, sewage decomposition is the primary contributor to NH_4^+. However, nitrification within the aquifer can partially explain the low NH_4^+ and NO_2^- concentrations and the weak correlations between NH_4^+ and increasing NO_3^- values along the flow paths (r = −0.57 to 0.30) (Table S4, Supplementary Fig. S4).

Table 3
Comparison of nitrate and chloride values in samples located near Forest/grasslands, Agricultural/urban areas, and Urban areas for groundwater in the Barva aquifer, Central Valley, Costa Rica.

Parameter	Statistic	Subregional LULC/Altitudinal section		
		Forest/ Grassland	Agriculture/ Urban	Urban
		***n* = 90**	***n* = 114**	***n* = 270**
NO_3^- [mg/L]	**Min**	0,3	9,5	9,1
	Median	1,8	27,8	27,9
	Max	7,6	110,7	47,5
	SD	1,5	16,4	7,7
	CV (%)	0,6	0,6	0,3
MW* p-value	**Forest/ Grassland**	1	**<0.0001**	0,289
	Agriculture/ Urban	**<0.0001**	1	**<0.0001**
	Urban	0,289	**<0.0001**	1
Cl^- [mg/L]	**Min**	0,9	2,8	4,7
	Median	1,6	4,9	9,9
	Max	3,3	24,5	24,6
	SD	0,5	3,6	4,8
	CV (%)	0,3	0,5	0,4
MW* p-value	**Forest/ Grassland**	1	**<0.0001**	**<0.0001**
	Agriculture/ Urban	**<0.0001**	1	**<0.0001**
	Urban	**<0.0001**	**<0.0001**	1

Values in bold show significant differences at a p-value <0.05.
* MW: Mann Whitney U test, CV: coefficient of variation.

5.3. NO_3^- sources in Barva aquifer using hydrochemical evolution

5.3.1. Bicarbonate excess with respect to anorthite hydrolysis

The bicarbonate excess relative to anorthite hydrolysis may indicate wastewater percolation. Madrigal-Solís et al. (2022) proposed that the dissolution of CO_2 from rainwater, the decomposition of OM, and the weathering of plagioclases and other aluminosilicate minerals increase H_2CO_3 and HCO_3^- levels in the Barva aquifer. Additionally, the possibility of volcanic CO_2 entering the groundwater, although limited, cannot be dismissed. Despite the Barva volcano exhibiting low activity (Arredondo Li and Soto, 2007), with no observed degassing or CO_2 emissions (Aiuppa et al., 2014), it is considered a young volcano (Protti, 1986).

The excess of bicarbonate with respect to Ca^{2+} along the hydrolysis line of anorthite, particularly in the Barva south flow path and lower urban zones (Fig. 4d and f), suggests additional HCO_3^- sources, such as percolation from wastewater through septic tanks. In these areas, higher DOC indicates that wastewater percolation could release HCO_3^- due to OM mineralization, as suggested in a study in Tunisia (Ben Messaoud et al., 2021).

Samples positioned above the 1:2 hydrolysis equiline of anorthite in the Ca^{2+}: HCO_3^- bivariable plot support this hypothesis, following the equation:

$$CaAl_2Si_2O_8\ (\text{anorthite}) + 2CO_2 + 3H_2O \rightarrow Al_2Si_2O_5(OH)_4\ (\text{kaolinite}) + Ca^{2+} + 2HCO_3^- \quad (2)$$

Therefore, a portion of the excess of HCO_3^-, beyond what is expected from anorthite hydrolysis, may partly be attributed to wastewater percolation. Denitrification, which can also release HCO_3^- along with the oxidation of DOC (McMahon and Chapelle, 2008), is unlikely as a widespread process in the Barva aquifer due to high DO and Eh levels.

5.3.2. Cl^- and Na^+ correlations

The Cl^- and Na^+ correlations serve as reliable indicators of anthropogenic contamination in the area, given the low Cl^- content in volcanic lithology (Custodio and Llamas, 1983). Strong correlations between Cl^- and Na^+ along the Barva aquifer flow paths, with samples near or above the 1:1 equiline in the Na^+ and Cl^- bivariable plot (Fig. 4f), suggest anthropogenic sources, including KCl fertilizer application and the leaching of chlorinated salts from domestic sewage (Cao et al., 2022), alongside the hydrolysis of Na^+ from Na^+-rich plagioclases (Madrigal-Solís et al., 2022). The stronger correlation found in the south flow path ($r = 0.91$) indicates a greater impact from sewage as groundwater passes beneath major cities. Samples below the equiline show lesser influence from KCl and lower Cl^- concentrations, which traverses more agricultural areas (Figs. 1 and 2). Samples near and above the 1:1 equiline also correspond to sites with the highest NO_3^- levels within the Agricultural/urban and Urban LULC sectors, confirming the anthropogenic origin of Cl^- contents.

5.3.3. Adsorption and leaching of NH_4^+, Ca^{2+} and NO_3^- in variable-charged Andisols

Higher positive correlations were observed between Ca^{2+} and NO_3^- concentrations in samples from the Agricultural/urban zone ($r = 0.78$) compared to forested ($r = 0.42$) and urban areas ($r = 0.48$) (Table S5). Ca^{2+} concentrations in the Barva aquifer, particularly in the middle and lower zones, are higher than those in the Colima aquifers, despite the latter experiencing longer transit times and higher mineralization (Madrigal-Solís et al., 2022). Both aquifer systems contain abundant Ca^{2+}-rich plagioclases, primarily anorthite. In coffee plantations, Ca^{2+} is applied through liming rather than Ca^{2+}-enriched fertilizers (ICAFE, 2020; MMARN, 2021). Thus, two hypotheses for the higher Ca^{2+} contents in the Barva aquifer and the strong correlation between Ca^{2+} and NO_3^- in agricultural areas were proposed: leaching from anthropogenic activities, such as lime application and Ca^{2+} normal exchange in the Colima aquifers.

Acid and variable-charged Andisols have high anion exchange capacity (AEC) and low to moderate cation exchange capacity (CEC) (Anda and Dahlgren, 2020; Auxtero et al., 2004). Andisols with high allophane, inorganic clays, particularly kaolinite, and Al/Fe oxides exhibit lower CEC and higher AEC compared to those with more humus and silicate minerals (Auxtero et al., 2004; Brady and Weil, 2002). In the Central Valley, vitric-allophanic-halloysitic Andisols have reduced cation retention, favoring leaching due to high precipitation rates (Alvarado et al., 2014). However, liming can modify the CEC and AEC in Andisols (Auxtero et al., 2004; Fiantis et al., 2002).

Liming amendments, mainly as calcite ($CaCO_3$), are used in coffee plantations to counteract soil acidification from acidic Andisols, heavy rainfall, and ammoniacal N-fertilizers (Brizzolara, 2020; ICAFE, 2020; Reynolds-Vargas et al., 1994). This process introduces Ca^{2+} into the soil solution, yet leaching is mainly restricted to the first centimeters below the application depth (McDaniel et al., 2012). As lime increases pH, it lowers the point of zero charge (PZC), increases the CEC (Anda and Dahlgren, 2020; Auxtero et al., 2004), and facilitates Ca^{2+} replacing aluminum at binding sites (Olego et al., 2021; Ernani et al., 2004). Despite their high buffering capacity, which makes raising soil pH difficult (Espinosa and Molina, 2015; Fiantis et al., 2002), these soils still show an increase in CEC (Acosta et al., 2020; Mora et al., 2002, 1999), even at low pH.

Although liming generally increases CEC, Ca^{2+} leaching remains plausible. Insufficient liming in agricultural areas or the absence in urban areas might limit CEC enhancement and Ca^{2+} retention. In nearby zones, lime applications for andesitic soils often fall below recommended levels due to difficulties in dose estimation or resistance from farmers (Brizzolara, 2020). This may result in persistently low to moderate CEC and potential Ca^{2+} leaching. A study in southern Costa Rica showed limited soil Ca^{2+} after the application of dolomitic lime, suggesting lower retention by soil particles in Andisols compared to other nutrients (Henriquez and Bertsch, 1997).

The pH-dependent AEC in acid Andisols favors moderate NO_3^- adsorption, but oversaturation of positive charges can lead to NO_3^-

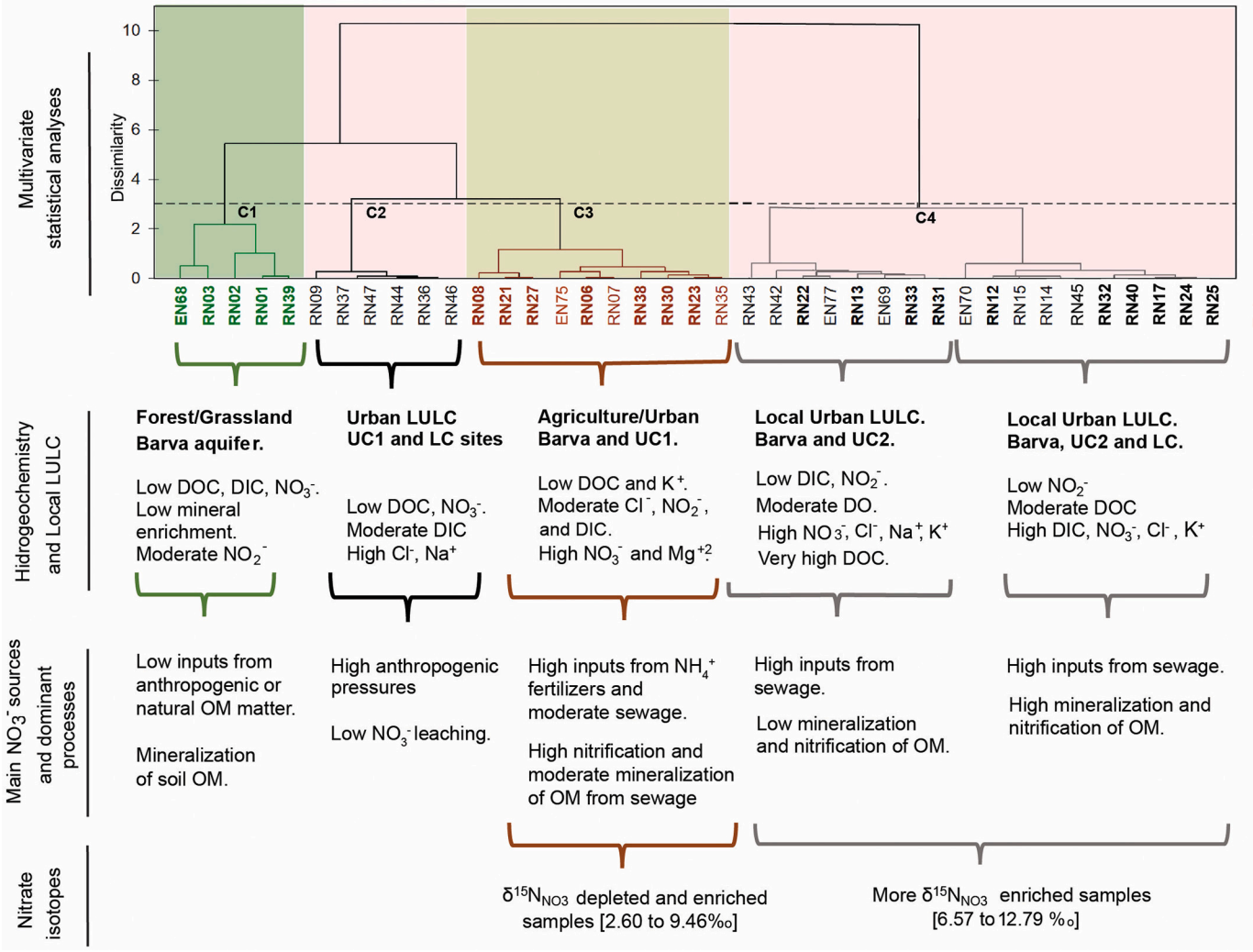

Fig. 7. Hierarchical Cluster Analysis (HCA)-based clustering of sites in Barva and Colima aquifers, utilizing hydrochemical variables while excluding NO_3^- isotopes. The figure portrays land use and land cover within each cluster, primary hydrogeochemical characteristics, main NO_3^- sources, dominant biochemical processes, and results from NO_3^- isotopes for cluster validation.

leaching into the Barva aquifer (Cannavo et al., 2013; Ryan et al., 2001; Reynolds-Vargas et al., 1994). Increasing CEC during liming reduces AEC, intensifying anion leaching and NO_3^- groundwater pollution in the Agricultural/urban zone. Thus, the strong Ca^{2+} vs. NO_3^- correlation in agricultural areas may result from ammoniacal fertilizer leaching and weathering of calcium-rich plagioclases (Madrigal-Solís et al., 2022), with a portion of Ca^{2+} leaching from agricultural amendments. In contrast, Ca^{2+} vs. NO_3^- correlations in urban areas remain negligible. Other studies have also used such correlations to indicate agricultural impacts on groundwater in non-Andisols soils (Maurya et al., 2021; Minet et al., 2017). Moreover, the hypothesis of normal ion exchange, with Ca^{2+} adsorbed in Colima aquifers, may also explain higher Ca^{2+} contents in the Barva aquifer.

Likewise, NH_4^+ adsorption by soil particles can delay its entry into groundwater (Böhlke et al., 2006; Nikolenko et al., 2018). Nitrification and variations in cation and anion retention rates in Andisols, influenced by the pH-dependent PZC, may explain the low concentrations of NH_4^+ and the low correlations between NH_4^+ and NO_3^- in the study area (Table S4, Fig. S4).

5.4. DOC and $\delta^{15}N_{NO3}$ for identifying NO_3^- sources in Barva aquifer across LULC patterns

The area exhibits distinct zoning in LULC patterns, supporting the hypothesis that NO_3^- in agricultural/urban zones, contributing an estimated 16 % of wastewater, is primarily attributable to N-fertilizer application. Overall, samples located in the agricultural/urban sector showed $\delta^{15}N_{NO3}$ values ranging from +2.6 to +9.5 ‰, falling within the overlapped ranges for NO_3^- from N-fertilizer, soil organic nitrogen, and sewage (Kendall, 1998; Xue et al., 2009) (Fig. 5a). However, significantly lower DOC values in these samples compared to the Urban LULC (Fig. 5b) suggest a lower influence of OM from sewage. Thus, in this agriculture-dominated region, NO_3^- concentrations from 9.5 to 110.7 mg/L (Fig. 3a-b, Table 3), are primarily influenced by N-fertilizers.

In contrast, sites located within the Urban LULC region showed $\delta^{15}N_{NO3}$ values ranging from +7.2 to +11 ‰, within the expected overlapping ranges for soil organic nitrogen and sewage (Fig. 5a). Groundwater in this urban sector displayed elevated levels of DOC and NO_3^- contents, from 9.1 to 47.5 mg/L (Fig. 3a, e), implying infiltration of wastewater from septic tanks and sewerage system leakages, with NO_3^- originating after mineralization and nitrification processes. Moreover, 80 % of wastewater is estimated to originate from the urban sector.

5.5. Zoning of NO_3^- sources in Barva aquifer based on HCA and PCA analyses

The significant contribution of DOC and other hydrochemical parameters in identifying NO_3^- sources in each LULC sector was demonstrated by comparing PCAs and HCA results, with and without $\delta^{15}N_{NO3}$ information (Fig. 6a-d). Fig. 7 summarizes essential hydrochemical and LULC patterns, primary NO_3^- sources, dominant processes, and associated NO_3^- isotopic ranges within four sample groups. HCA in Fig. 7 comprised only hydrochemical parameters and all samples from the Barva and Colima aquifers.

In the Forest/Grassland LULC clusters (Figs. 6c-d and 7), sites show low levels of major ions, DOC, DIC, and NO_3^- (5.1 ± 4.3 mg/L) (Fig. 3), indicating minor anthropogenic pollution. However, a moderate correlation between NO_3^- and Cl^- ($r = 0.71$) might signal incipient leaching of NO_3^- from sewage or fertilizers, while high correlations among Ca^{2+} vs. Na^+, Mg^{2+}, and HCO_3^- ($r = 0.74$ to 0.89) (Table S5) suggest weathering of Na^+ and Ca^{2+}-rich plagioclases (Madrigal-Solís et al., 2022). In this area, OM from sewage or animal farms is not a significant source of NO_3^-, given the absence of population centers, low density of farms (Fig. 2; Madrigal-Solís et al., 2014), and the uncommon practice of organic fertilization with manure (Infante-Amate and Picado, 2018; San Martin Ruiz et al., 2021).

In the Agricultural/urban LULC clusters, low DOC, $\delta^{15}N_{NO3}$, and K^+ values, moderate Cl-, NO_2^- and DIC, and elevated NO_3^- contents may indicate dominant percolation of inorganic N-fertilizers, commonly used in coffee plantations (ICAFE, 2020) (Figs. 6a-d and 7). Moreover, a secondary contribution from sewage inputs is plausible, which might undergo rapid mineralization and nitrification, potentially reducing DOC levels.

Increased correlations between NO_3^- vs. Ca^{2+} ($r = 0.81$) (see section 5.3), Ca^{2+} vs. Cl^- and Ca^{2+} vs Mg^{2+} ($r = 0.83$ and 0.94), and Mg^{2+} vs. Cl^- ($r = 0.76$) imply the influence of agricultural activities. Mineral weathering (Madrigal-Solís et al., 2022) and the application of urea, NH_4NO_3, potassium chloride (KCl), and magnesium oxide (MgO)-rich fertilizers in coffee cultivation zones (Castro-Tanzi et al., 2012; ICAFE, 2020) may partially explain these positive correlations. Other studies have also related positive correlations between NO_3^-, Ca^{2+}, Cl^-, and Mg^{2+} with agricultural activities (Cao et al., 2022; Maurya et al., 2021). High correlations between Na^+ vs. Cl^- and NO_3^- vs. Cl^- (Table S5) might also indicate the influx of KCl and N-fertilizers (Minet et al., 2017).

Sites RN27 and RN32 in this Agriculture/urban sector showed $\delta^{15}N_{NO3}$ values within the range for domestic sewage (9.5 and 10‰, respectively) (Xue et al., 2009; Kendall et al., 2007), potentially masked by rapid leaching of OM from septic tanks or damaged sewerage systems nearby. Thus, local Urban LULC around RN27 and 32 might lead to underestimating the impact of fertilization in the regional upstream watershed (Fig. 2).

In the Urban LULC clusters, samples are characterized by similar NO_3^- concentrations and higher $\delta^{15}N_{NO3}$, DOC, DIC, and K^+ values compared to the Agricultural/urban sector, suggesting increased sewage infiltration (Figs. 6a-d and 7). The strong associations between $\delta^{15}N_{NO3}$, NO_3^-, Cl^-, K^+, Na^+, Ca^{2+}, and DOC, as indicated by the PCA results of Barva aquifer samples (Fig. 6a, c) and the strong correlation between NO_3^- and Cl^- ($r = 0.73$), further support sewage percolation as the primary source of pollution. Elevated K^+ (Fig. 6e), found in many detergents, decomposing OM, and sewage (Arumugam et al., 2023; Huang et al., 2022; Minet et al., 2017; Cao et al., 2022;), along with high $\delta^{15}N_{NO3}$ and DOC values also support sewage percolation as the primary source of pollution in the urban sector, agreeing with the findings reported by Reynolds-Vargas et al. (2006). Samples in the Urban LULC sector showed two subgroupings of samples: those with moderate DOC and those with the highest DOC levels. The latter may imply continuous OM influx from nearby septic systems or sewage seepages. Diminished groundwater velocity near RN13, 22, 31, and 33 (Supplementary Fig. S1a), linked to a reduced hydraulic gradient, could extend OM residence time, resulting in higher DOC concentrations.

The PCA and HCA analyses reveal that DOC and other hydrochemical parameters are adequate indicators of environmental pressures on water quality, independently of the inclusion of $\delta^{15}N_{NO3}$ information (Figs. 6 and 7). This is particularly useful in areas with limited application of organic fertilizers, such as Central Valley (Infante-Amate and Picado, 2018; San Martin Ruiz et al., 2021). Consistent oxidizing conditions across the Barva aquifer (Fig. 4b and Supplementary Fig. S3a) support the hypothesis that higher DOC in urban areas (Fig. 3e) are due to the leaching of larger amounts of OM from population centers rather than higher decomposition rates in agricultural areas.

Fig. 8 shows the zoning of sectors under the influence of dominant NO_3^- sources in the study area, based on multivariate statistical analyses (Figs. 6 and 7) and supported by $\delta^{15}N_{NO3}$, DOC, and other hydrochemical parameters (Figs. 3e, 4a and 5b). The map shows areas primarily influenced by soil organic matter, N-fertilizers, and sewage, with site clusters identified through HCA. Analyses indicate that inorganic N-fertilizers are a significant source of contamination, comparable to wastewater in terms of NO_3^- concentrations (Table 3) and the extent of affected areas in agricultural and urban LULC sectors (Fig. 8). This finding contrasts with a previous study using dual NO_3^- isotopes and Bayesian mixing analysis, which estimated only 2.9 % and 14.4 % average contributions from fertilizers in wells and springs, respectively (Sánchez-Gutiérrez et al., 2023). The discrepancy may be due to uncertainties in source identification using dual NO_3^- isotopes and Bayesian mixing models, caused by overlapping $\delta^{15}N_{NO3}$ ranges (between N- fertilizers, soil OM, sewage, and manure), isotopic fractionation, and mixing of multiple NO_3^- sources (Kendall et al., 2007; Xue et al., 2009; Choi et al., 2017).

Finally, the contribution of the NO_3^- from ammoniacal fertilizers may be underestimated in the lower zone. The typical depleted $\delta^{15}N_{NO3}$ signal of these fertilizers diminishes or disappears due to a significant influx of wastewater in urban areas, which is estimated to account for about 80 % of total wastewater discharge in the study area. This wastewater-derived NO_3^- masks the fertilizer signal by mixing with $\delta^{15}N_{NO3}$-enriched NO_3^-, resulting in enriched signals in the lower urban zone. Dilution from high precipitation rates may further diminish the fertilizer signal along the flow path. Additionally, nitrification of NH_4-fertilizers, which are the predominant N-fertilizers in the study area, may generate new enriched NO_3^- in groundwater (Kendall, 1998).

5.6. Pollution and biochemical processes in Colima aquifers

Elevated DO and Eh values in Upper and Lower Colima aquifers, similar to those in the Barva aquifer (Table 1, Fig. 4b), suggest general oxidating conditions. DO is the preferred electron acceptor by microorganisms, leading to its consumption along flow paths, particularly in isolated aquifers (McMahon and Chapelle, 2008). Despite the Colima aquifers being confined and semiconfined, hydraulic connections with the Barva aquifer through fractured Tiribí formation (BGS/SENARA, 1988; Madrigal-Solís et al., 2022) or DO enrichment during recharge in the unconfined sectors may maintain relatively high DO levels. The oxidizing conditions can favor mineralization and nitrification processes, despite the biplot of $\ln(NO_3^-)$ vs. $\delta^{15}N_{NO3}$ (Fig. 5c) not revealing a linear relationship among the Colima sites, while also hindering denitrification.

Anthropogenic activities and groundwater mixing modify hydrogeochemical evolution along Colima aquifer flow paths. The Upper Colima southern path displays the highest NO_3^- values (10.8 to 58.5 mg/L), largely due to mixing with the Barva south flow path. Both Upper Colima paths show low correlations between physicochemical constituents and distance, except for increasing HCO_3^-, likely due to varying degrees of confinement and anthropogenic pressures (Fig. 2). In the confined Lower Colima aquifer, most components decrease towards the discharge zone, except for NO_3^- ($r = 0.88$), indicating mixing with the Upper Colima south flow path.

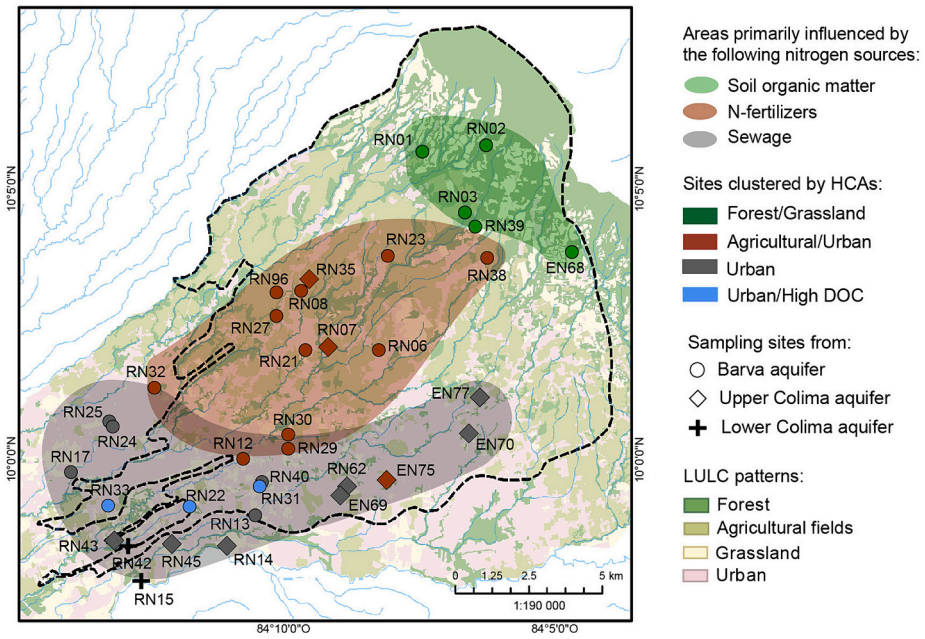

Fig. 8. Zoning of sectors under the influence of dominant NO_3^- sources in the study area, based on multivariate statistical analyses and supported by $\delta^{15}N_{NO3}$, DOC, and other hydrochemical parameters. The map shows areas primarily influenced by soil organic matter, N-fertilizers, and sewage, with site clusters identified through hierarchical cluster analysis (HCA).

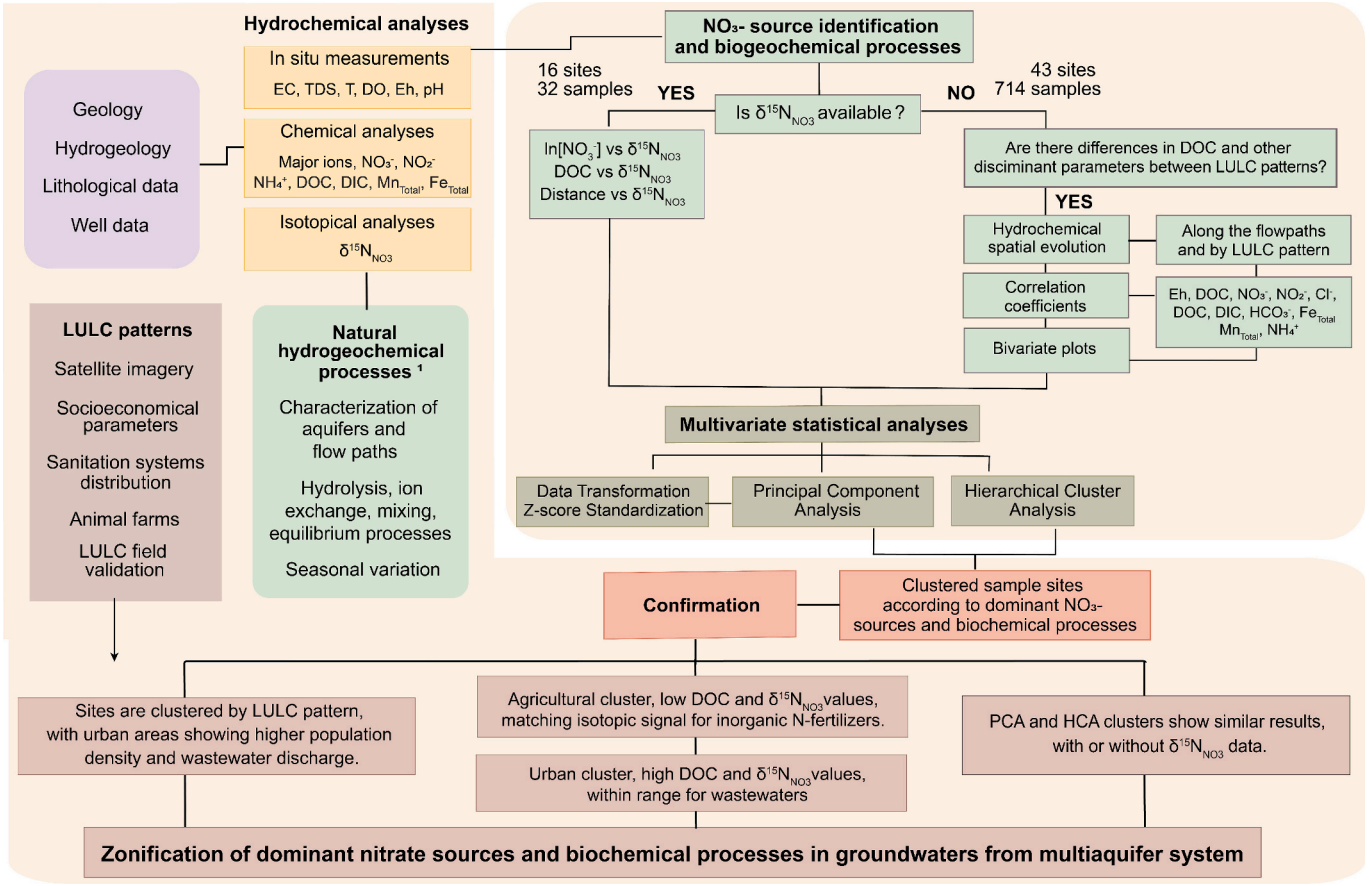

Fig. 9. Methodological approach to trace NO_3^- origins and biogeochemical processes in groundwater, with and without $\delta^{15}N_{NO3}$ isotopic analysis. [1] Madrigal-Solís et al. (2022).

PCA and HCA analyses, with and without $\delta^{15}N_{NO3}$ information, accurately grouped Colima sampling sites based on regional LULC (Figs. 6a-b, 7 and 8). In Fig. 7, sites in the urban sector (C2) with low NO_3^- and DOC values indicate low anthropogenic contamination possibly due to a higher local confinement in the surrounding area. In the Agricultural/Urban zone (C3), low DOC and $\delta^{15}N_{NO3}$ values ranging (from +3.8 to +4.7 ‰), within the ranges associated with ammoniacal fertilizers (Kendall et al., 2007; Xue et al., 2009), suggest N-fertilizer nitrification is the main NO_3^- source (Fig. 7). In contrast, higher NO_3^-, DOC, and enriched $\delta^{15}N_{NO3}$ values (from +8.4 to +11.0 ‰) (Table S3) in Urban clusters indicate sewage pollution, particularly in the discharging zone (Fig. 6a-b and Fig. 7).

5.7. Graphical representation of the proposed method for identifying NO_3^- sources

The chart in Fig. 9 illustrates the proposed methodology for identifying NO_3^- contamination sources, such as N-fertilizers and sewage, and biogeochemical processes in groundwater. This approach integrates diverse data types, including socio-economic parameters, LULC, hydrogeology, hydrochemical analyses, isotopic data, and multivariate statistical analyses, providing a thorough understanding of contamination processes, particularly when dealing with extensive environmental data. By incorporating DOC and other hydrochemical indicators, it remains robust even in regions with limited $\delta^{15}N_{NO3}$ data, making it applicable in resource-limited settings. For instance, sampling 43 sites for hydrochemical analyses and only 16 for isotopic analyses effectively validated NO_3^- sources and biogeochemical processes at regional and local scales. Its successful application in the Barva and Colima aquifers demonstrates its potential for use in other regions.

This methodology can also serve as an alternative or complement to Bayesian mixing analyses, corroborating results from these models. The multi-faceted approach not only differentiates contamination sources but also generates zoning of sectors under specific NO_3^- contamination influences, facilitating targeted NO_3^- mitigation measures according to the contamination sources in each sector.

6. Conclusions

The extensive monitoring (2015–2022) of the Barva and Colima aquifers has revealed elevated NO_3^- concentrations surpassing international standards for human consumption in the middle and lower zones. Consistent DO and Eh values, low NH_4^+, NO_2-, Fe_{total}, and Mn_{total} concentrations, and an increase of DIC and NO_3^- along Barva flow paths, indicate that oxidizing conditions hinder denitrification. These findings confirm mineralization and nitrification as the primary biogeochemical processes in the four aquifers under study.

Groundwater from Forest/Grassland LULC sectors shows very low NO_3^-, low wastewater discharge, low DOC, and thus, minimal anthropogenic impact. In contrast, agricultural/urban zones display high NO_3^-, low wastewater discharge, low DOC, and depleted $\delta^{15}N_{NO3}$ values, indicating N-fertilizer percolation and ongoing contamination from agricultural practices. Urban areas, where almost 80 % of wastewater is generated, have high DOC and enriched $\delta^{15}N_{NO3}$ values, suggesting wastewater as the main NO_3^- source.

The analysis along Barva flow paths indicates distinct sources of contamination: higher fertilizer impact in the north path and a more significant sewage influence in the south. The north path features higher NO_3^-, a higher Cl^- to Na^+ ratio, and reduced HCO_3^- excess, indicating the impact of N and KCl fertilizer. In contrast, the south path shows signs of wastewater percolation. This aligns with the north path running beneath agricultural areas and the south path under urban centers. Differentiating flow paths helps to understand the connections between the Barva and Upper Colima south flow paths, both of which exhibit high NO_3^- and DOC, indicating wastewater percolation near populated centers. Thus, locally confined Upper Colima groundwater quality is also affected by land use.

This study presents a practical and cost-effective method for identifying and zoning dominant NO_3^- sources and biogeochemical processes without relying on nitrogen isotopic data. This approach is also suitable for regions with limited resources, facilitating the analysis of a larger number of sampling sites and samples. It provides similar results whether isotopes are used or not, enabling conclusions to be drawn with fewer or no samples for $\delta^{15}N_{NO3}$ analyses. It shows the effectiveness of multivariate statistics combined with DOC and other hydrogeochemical and socio-economical parameters in identifying NO_3^- sources in mixed urban-agricultural areas, especially in regions relying on synthetic fertilizers. These findings are essential for environmental management and groundwater protection, as they revealed a significant agricultural impact previously underestimated by nitrate isotopic Bayesian models in the study area.

7. Recommendations

For resource-limited countries, the methodology demonstrated in this study offers significant advantages. By prioritizing hydrochemical parameters and limiting isotopic analyses to a subset of sites, it is possible to study larger aquifer regions with a higher density of sites for more detailed assessments. Implementing this strategy in systematic monitoring programs will maximize resource efficiency and improve the understanding of groundwater contamination processes. To enhance groundwater contamination research, advanced techniques such as ^{13}C and ^{11}B isotope analyses are recommended, along with the assessment of heavy metals and emerging contaminants. Expanding DOC sampling campaigns and applying dual NO_3^- isotopic Bayesian analyses across a broader range of sites in agricultural and urban areas are also suggested.

Based on the conclusions of this study, implementing policies and regulations to reduce NO_3^- contamination related to N-fertilizer use in agricultural areas is needed in the Central Valley, Costa Rica. Key measures include optimizing fertilizer application and using slow-release fertilizers. In urban areas, prioritizing outdated sewage systems, expanding sewer infrastructure, and improving the design, maintenance, and technology of septic systems will reduce contamination from wastewater. A robust groundwater monitoring program and real-time monitoring systems are vital for detecting areas with considerable increases in NO_3^-. Public awareness campaigns are needed to educate residents and farmers on responsible practices. Collaboration among local authorities, environmental agencies, farmers, and community organizations, along with seeking funding and technical support from governmental and non-governmental organizations, is imperative to collectively address these issues and protect groundwater quality, the environment, and public health.

Funding

This project was supported by project numbers SIA 0291-13, 0045-18, and the “Laboratorio de Análisis Ambiental”, Universidad Nacional, Costa Rica. Additional support was obtained though Research Groups RNM-308 and RNM-128, sponsored by the “Junta de Andalucía”.

CRediT authorship contribution statement

Helga Madrigal-Solís: Writing – review & editing, Writing – original draft, Visualization, Supervision, Resources, Project administration, Methodology, Investigation, Funding acquisition, Formal analysis, Data curation, Conceptualization. **Iñaki Vadillo-Pérez:** Writing – review & editing, Supervision, Methodology, Investigation, Conceptualization. **Pablo Jiménez-Gavilán:** Writing – review & editing, Supervision, Methodology, Investigation, Conceptualization. **Alicia Fonseca-Sánchez:** Resources, Methodology, Investigation, Funding acquisition, Conceptualization. **Luis Quesada-Hernández:** Visualization, Formal analysis, Data curation. **Hazel Calderón-Sánchez:** Investigation. **Alicia**

Gómez-Cruz: Investigation. **Jorge Herrera Murillo:** Resources, Investigation, Conceptualization. **Roy Pérez Salazar:** Resources, Investigation.

Declaration of generative AI and AI-assisted technologies in the writing process

During the preparation of this work, the authors used ChatGPT to improve language and readability. After using this tool/service, the authors reviewed and edited the content as needed and take full responsibility for the content of the publication.

Declaration of competing interest

The authors disclose any competing financial interests or personal relationships that might be considered potential competing interests.

Data availability

Data will be made available on request.

Acknowledgments

The authors express their gratitude for the support extended by Empresa de Servicios Públicos de Heredia, ESPH S.A. (Costa Rica), in supplying lithological data from the boreholes managed by the corporation and collaborating on the collection of samples from specified wells.

Appendix A. Supplementary data

Supplementary data to this article can be found online at https://doi.org/10.1016/j.scitotenv.2024.174996.

References

Abascal, E., Gómez-Coma, L., Ortiz, I., Ortiz, A., 2022. Global diagnosis of nitrate pollution in groundwater and review of removal technologies. Sci. Total Environ. 810, 152233 https://doi.org/10.1016/j.scitotenv.2021.152233.

Acosta, D.F., Camacho Torres, Y.M., López Barón, C.A., Celyreyes, G.E., Serrano, P., 2020. Transformación electroquímica de un andisol en relación con la dinámica del fósforo. Biotecnol. Sect. Agropecuario Agroindustrial 18 (2), 94. https://doi.org/10.18684/BSAA(18)94-102.

Addinsoft, 2023. *XLSTAT* (2023.2.2) [Software]. https://www.xlstat.com/.

Aiuppa, A., Robidoux, P., Tamburello, G., Conde, V., Galle, B., Avard, G., Bagnato, E., De Moor, J.M., Martínez, M., Muñóz, A., 2014. Gas measurements from the Costa Rica–Nicaragua volcanic segment suggest possible along-arc variations in volcanic gas chemistry. Earth Planet. Sci. Lett. 407, 134–147. https://doi.org/10.1016/j.epsl.2014.09.041.

Alvarado, A., Mata, R., Chinchilla, M., 2014. Arcillas identificadas en suelos de Costa Rica a nivel generalizado durante el período 1931-2014: I. historia, metodología de análisis y mineralogía de arcillas en suelos derivados de cenizas volcánicas. Agron. Costarricense 38 (1), 75–106. https://doi.org/10.15517/rac.v38i1.15160.

American Public Health Association, 2005. In: Eaton, A.D. (Ed.), Standard Methods for the Examination of Water and Wastewater, 21st Ed. American Public Health Association, American Water Works Association, Water Environment Federation.

American Public Health Association, 2012. In: Rice, E.W., Baird, R.B., Eaton, A.D., Clesceri, L.S. (Eds.), Standard Methods for the Examination of Water and Wastewater, 22nd Ed. American Public Health Association, American Water Works Association, Water Environment Federation.

American Public Health Association, 2017. Standard Methods for the Examination of Water and Wastewater, 23rd ed. American Public Health Association, American Water Works Association, Water Environment Federation.

Anda, M., Dahlgren, R.A., 2020. Mineralogical and surface charge characteristics of andosols experiencing long-term, land-use change in West Java, Indonesia. Soil Sci. Plant Nutr. 66 (5), 702–713. https://doi.org/10.1080/00380768.2020.1820758.

Aravena, R., Robertson, W.D., 1998. Use of multiple isotope tracers to evaluate denitrification in ground water: study of nitrate from a large-flux septic system plume. Ground Water 36 (6), 975–982. https://doi.org/10.1111/j.1745-6584.1998.tb02104.x.

Aravena, R., Evans, M.L., Cherry, J.A., 1993. Stable isotopes of oxygen and nitrogen in source identification of nitrate from septic systems. Ground Water 31 (2), 180–186. https://doi.org/10.1111/j.1745-6584.1993.tb01809.x.

Arias-Salguero, M., Losilla-Penón, M., Arredondo-Li, S., 2006. Estado del conocimiento del agua subterránea en Costa Rica. Bol. Geol. Miner. 117 (1), 63–73.

Arredondo Li, S., Soto, G., 2007. Edad de las lavas del miembro los bambinos y sumario cronoestratigráfico de la Formación Barva, Costa Rica. Rev. Geol. Am. Cent. 34-35, 59–71. https://doi.org/10.15517/rgac.v0i34-35.4226.

Arumugam, T., Kinattinkara, S., Kannithottathil, S., Velusamy, S., Krishna, M., Shanmugamoorthy, M., Sivakumar, V., Boobalakrishnan, K.V., 2023. Comparative assessment of groundwater quality indices of Kannur District, Kerala, India using multivariate statistical approaches and GIS. Environ. Monit. Assess. 195 (1), 29. https://doi.org/10.1007/s10661-022-10538-2.

Auxtero, E., Madeira, M., Sousa, E., 2004. Variable charge characteristics of selected Andisols from the Azores, Portugal. Catena 56 (1–3), 111–125. https://doi.org/10.1016/j.catena.2003.10.006.

Ben Messaoud, R., Lachaal, F., Leduc, C., Mlayah, A., 2021. Discharge of treated wastewater: hydrodynamic and hydrogeochemical impacts on the Kairouan plain aquifer (Central Tunisia). Environ. Earth Sci. 80 (10), 381. https://doi.org/10.1007/s12665-021-09667-7.

BGS/SENARA, 1988. The Continuation of Hydrogeological Investigations in the North and East of the Valle Central, Costa Rica. Final Report 1984-1987. (Technical Report WD/88/13R). British Geological Survey, p. 120.

Böhlke, J.K., Smith, R.L., Miller, D.N., 2006. Ammonium transport and reaction in contaminated groundwater: application of isotope tracers and isotope fractionation studies: NH_4^+ TRANSPORT IN CONTAMINATED GROUNDWATER. Water Resour. Res. 42 (5) https://doi.org/10.1029/2005WR004349.

Bower, K.M., 2014. Water supply and sanitation of Costa Rica. Environ. Earth Sci. 71 (1), 107–123. https://doi.org/10.1007/s12665-013-2416-x.

Brady, N.C., Weil, R.R., 2002. The Nature and Properties of Soils, 13.a ed. Prentice Hall.

Brizzolara, D., 2020. Soil Fertility in an Acidic Andisol: An Analysis of Acidity Management Practices in Vara Blanca, Costa Rica. Point Loma Nazarene University.

Cannavo, P., Harmand, J.-M., Zeller, B., Vaast, P., Ramírez, J.E., Dambrine, E., 2013. Low nitrogen use efficiency and high nitrate leaching in a highly fertilized Coffea arabica–Inga densiflora agroforestry system: A 15N labeled fertilizer study. Nutr. Cycl. Agroecosyst. 95 (3), 377–394. https://doi.org/10.1007/s10705-013-9571-z.

Cao, X., Shi, Y., He, W., An, T., Chen, X., Zhang, Z., Liu, F., Zhao, Y., Zhou, P., Chen, C., He, J., He, W., 2022. Impacts of anthropogenic groundwater recharge (AGR) on nitrate dynamics in a phreatic aquifer revealed by hydrochemical and isotopic technologies. Sci. Total Environ. 839, 156187 https://doi.org/10.1016/j.scitotenv.2022.156187.

Castro-Tanzi, S., Dietsch, T., Urena, N., Vindas, L., Chandler, M., 2012. Analysis of management and site factors to improve the sustainability of smallholder coffee production in Tarrazú, Costa Rica. Agr Ecosyst Environ 155, 172–181. https://doi.org/10.1016/j.agee.2012.04.013.

Choi, W.-J., Kwak, J.-H., Lim, S.-S., Park, H.-J., Chang, S.X., Lee, S.-M., Arshad, M.A., Yun, S.-I., Kim, H.-Y., 2017. Synthetic fertilizer and livestock manure differently affect δ15N in the agricultural landscape: A review. Agr Ecosyst Environ 237, 1–15. https://doi.org/10.1016/j.agee.2016.12.020.

Corp, I.B.M., 2021. *IBM SPSS Statistics for Macintosh* (28.0) [Software]. IBM Corp.

Custodio, E., Llamas, M.R., 1983. Hidrología subterránea, Vol. 2. Omega. https://www.academia.edu/41067940/Custodio_Llamas_Tomo.

Echandi, E., 1981. Unidades volcánicas de la vertiente norte del río Virilla [Licentiate Thesis]. University of Costa Rica.

Ernani, P.R., Ribeiro, M.F.S., Bayer, C., 2004. Chemical modifications caused by liming below the limed layer in a predominantly variable charge acid soil. Commun. Soil Sci. Plant Anal. 35 (5–6), 889–901. https://doi.org/10.1081/CSS-120030365.

Espinosa, J., Molina, E., 2015. Acidez y encalado de los suelos (Soil acidity and liming). International Plant Nutrition Institute. https://doi.org/10.13140/2.1.3888.9281.

Fiantis, D., Van Ranst, E., Shamshuddin, J., Fauziah, I., Zauyah, S., 2002. Effect of calcium silicate and superphosphate application on surface charge properties of volcanic soils from West Sumatra, Indonesia. Commun. Soil Sci. Plant Anal. 33 (11−12), 1887–1900. https://doi.org/10.1081/CSS-120004829.

Foster, S., Ellis, A.T., Losilla-Penon, M., Rodriguez-Estrada, H.V., 1985. Role of volcanic tuffs in ground-water regime of Valle central, Costa Rica. Ground Water 23 (6), 795–801. https://doi.org/10.1111/j.1745-6584.1985.tb01959.x.

Gan, L., Huang, G., Pei, L., Gan, Y., Liu, C., Yang, M., Han, D., Song, J., 2022. Distributions, origins, and health-risk assessment of nitrate in groundwater in typical alluvial-pluvial fans, North China plain. Environ. Sci. Pollut. Res. 29 (12), 17031–17048. https://doi.org/10.1007/s11356-021-17067-4.

Gao, Z., Weng, H., Guo, H., 2021. Unraveling influences of nitrogen cycling on arsenic enrichment in groundwater from the Hetao Basin using geochemical and multi-isotopic approaches. J. Hydrol. 595, 125981 https://doi.org/10.1016/j.jhydrol.2021.125981.

Gómez-Cruz, A., 1987. Evaluación del potencial de los acuíferos y diseño de las captaciones de agua subterránea en la zona de Puente de Mulas, provincia de Heredia, Costa Rica [Licentiate Thesis]. University of Costa Rica.

Gupta, T., Kumari, R., 2023. Source apportionment of groundwater quality in agriculture-dominated semiarid region, India—using an integrated approach of hydrochemistry, stable isotopes and land use/land cover change. Environ. Dev. Sustain. https://doi.org/10.1007/s10668-023-03744-6.

Hannah, R., Vogel, T.A., Patino, L.C., Alvarado, G.E., Perez, W., Smith, D.R., 2002. Origin of silicic volcanic rocks in Central Costa Rica: A study of a chemically variable ash-flow sheet in the Tiribí tuff. Bull. Volcanol. 64 (2), 117–133. https://doi.org/10.1007/s00445-001-0188-8.

Harris, S.J., Cendón, D.I., Hankin, S.I., Peterson, M.A., Xiao, S., Kelly, B.F.J., 2022. Isotopic evidence for nitrate sources and controls on denitrification in groundwater beneath an irrigated agricultural district. Sci. Total Environ. 817, 152606 https://doi.org/10.1016/j.scitotenv.2021.152606.

Hauptman, B.H., Naughton, C.C., Harmon, T.C., 2023. Using machine learning to predict 1,2,3-trichloropropane contamination from legacy non-point source pollution of

groundwater in California's Central Valley. Groundw. Sustain. Dev. 22, 100955 https://doi.org/10.1016/j.gsd.2023.100955.
He, S., Li, P., Su, F., Wang, D., Ren, X., 2022. Identification and apportionment of shallow groundwater nitrate pollution in Weining plain, Northwest China, using hydrochemical indices, nitrate stable isotopes, and the new Bayesian stable isotope mixing model (MixSIAR). Environ. Pollut. 298, 118852 https://doi.org/10.1016/j.envpol.2022.118852.
Henriquez, C., Bertsch, F., 1997. Comportamiento de Ca, Mg y K en respuesta a la aplicación de fertilizante potásico y de cal dolomítica en un andisol de la Zona Sur de Costa Rica. Agron. Costarricense 21 (2), 239–248.
Hosono, T., Alvarez, K., Lin, I.-T., Shimada, J., 2015. Nitrogen, carbon, and sulfur isotopic change during heterotrophic (pseudomonas aureofaciens) and autotrophic (Thiobacillus denitrificans) denitrification reactions. J. Contam. Hydrol. 183, 72–81. https://doi.org/10.1016/j.jconhyd.2015.10.009.
Huang, G., Liu, C., Sun, J., Zhang, M., Jing, J., Li, L., 2018. A regional scale investigation on factors controlling the groundwater chemistry of various aquifers in a rapidly urbanized area: A case study of the Pearl River Delta. Sci. Total Environ. 625, 510–518. https://doi.org/10.1016/j.scitotenv.2017.12.322.
Huang, G., Pei, L., Li, L., Liu, C., 2022. Natural background levels in groundwater in the Pearl River Delta after the rapid expansion of urbanization: A new pre-selection method. Sci. Total Environ. 813, 151890 https://doi.org/10.1016/j.scitotenv.2021.151890.
Huang, G., Hou, Q., Han, D., Liu, R., Song, J., 2023. Large scale occurrence of aluminium-rich shallow groundwater in the Pearl River Delta after the rapid urbanization: co-effects of anthropogenic and geogenic factors. J. Contam. Hydrol. 254, 104130 https://doi.org/10.1016/j.jconhyd.2022.104130.
ICAA, Ministerio de Ambiente y Energía, Ministerio de Salud, 2016. Política Nacional de Saneamiento en Aguas Residuales 2016–2045. https://www.aya.go.cr/Noticias/Documents/Politica%20Nacional%20de%20Saneamiento%20en%20Aguas%20Residuales%20marzo%202017.pdf.
ICAFE, 2020. Technical guide for coffee cultivation, 2.a Ed. In: Coffee Institute of Costa Rica (ICAFE)-coffee research Center of Costa Rica (CICAFE) https://www.icafe.cr/wp-content/uploads/cicafe/documentos/GUIA-TECNICA.pdf.
IICA, Dangelo, S.-C., Rafael, M.C., 2017. Digital soil map of Costa Rica. Inter-American Institute for Cooperation on Agriculture. https://repositorio.iica.int/handle/11324/8511?show=full.
IMN, 2014. Precipitación Anual 1960–2013. Sistema Nacional de Información Territorial (SNIT), Costa Rica. https://www.snitcr.go.cr/Visor/index2019?k=Y2FwYTo6SU1OOjphbnVhbF9wcmVfNjBfMTM.
INEC, 2018. Estadísticas demográficas. 2011–2025. Proyecciones nacionales. Población total proyectada al 30 de junio por grupos de edades, según región de planificación y sexo [XLSX]. http://inec.cr/poblacion/estimaciones-y-proyecciones-de-poblacion.
Infante-Amate, J., Picado, W., 2018. Energy flows in the coffee plantations of Costa Rica: from traditional to modern systems (1935–2010). Reg. Environ. Chang. 18 (4), 1059–1071. https://doi.org/10.1007/s10113-017-1263-9.
Ji, B., Yang, K., Zhu, L., Jiang, Y., Wang, H., Zhou, J., Zhang, H., 2015. Aerobic denitrification: A review of important advances of the last 30 years. Biotechnol. Bioprocess Eng. 20 (4), 643–651. https://doi.org/10.1007/s12257-015-0009-0.
Jurado, A., Borges, A.V., Brouyère, S., 2017. Dynamics and emissions of N2O in groundwater: A review. Sci. Total Environ. 584-585, 207–218. https://doi.org/10.1016/j.scitotenv.2017.01.127.
Kendall, C. (1998). Tracing nitrogen sources and cycling in catchments. En Isotope Tracers in Catchment Hydrology (1.ª ed., pp. 519–576). Elsevier Science.
Kendall, C., Elliott, E. M., & Wankel, S. D. (2007). Tracing anthropogenic inputs of nitrogen to ecosystems. En R. Michener & K. Lajtha (Eds.), Stable Isotopes in Ecology and Environmental Science (1.ª ed., pp. 375–449). Wiley. https://doi.org/10.1002/9780470691854.ch12.
Knoll, L., Breuer, L., Bach, M., 2019. Large scale prediction of groundwater nitrate concentrations from spatial data using machine learning. Sci. Total Environ. 668, 1317–1327. https://doi.org/10.1016/j.scitotenv.2019.03.045.
Kraft, B., Tegetmeyer, H.E., Sharma, R., Klotz, M.G., Ferdelman, T.G., Hettich, R.L., Geelhoed, J.S., Strous, M., 2014. The environmental controls that govern the end product of bacterial nitrate respiration. Science 345 (6197), 676–679. https://doi.org/10.1126/science.1254070.
Kussmaul, S., 1988. Comparación petrológica entre el piso volcánico del Valle Central y la Cordillera Central de Costa Rica. Rev. Cienc. Technol. 12 (1–2), 109–116.
Kussmaul, S., & Sprechmann, P. (1982). Estratigrafía de Costa Rica (América Central), II: Unidades litoestratigráficas Ígneas. En P. Sprechmann (Ed.), Manual de Geología de Costa Ric: Vol. 1:Estratigrafía 291-299). Universidad de Costa Rica.
Liu, X., Wang, X., Zhang, L., Fan, W., Yang, C., Li, E., Wang, Z., 2021. Impact of land use on shallow groundwater quality characteristics associated with human health risks in a typical agricultural area in Central China. Environ. Sci. Pollut. Res. 28 (2), 1712–1724. https://doi.org/10.1007/s11356-020-10492-x.
Losilla, M., Rodríguez, H., Schosinsky, G., Stimson, J., Bethune, D., 2001. Los acuíferos volcánicos y el desarrollo sostenible en América Central, 1. ed. Editorial de la Universidad de Costa Rica.
Madrigal-Solís, H., Fonseca-Sánchez, A., Núñez-Solís, Christian, Gómez-Cruz, Alicia, 2014. Amenaza de contaminación del agua subterránea en el sector norte del acuífero Barva, Heredia, Costa Rica [threat of groundwater contamination in the northern sector of the Barva aquifer, Heredia, Costa Rica]. Tecnol. Cienc. Agua 5 (6), 109–118.
Madrigal-Solís, H., Fonseca-Sánchez, A., Reynolds-Vargas, J., 2017. Caracterización hidrogeoquímica de los acuíferos volcánicos Barva y Colima en el Valle Central de Costa Rica. Tecnol. Cienc. Agua 08 (1), 115–132. https://doi.org/10.24850/j-tyca-2017-01-09.
Madrigal-Solís, H., Fonseca-Sánchez, A., Calderón-Sánchez, H., Gómez-Cruz, A., Núñez-Solís, C., 2019. Design of a monitoring network as a participative management tool: physical and chemical quality of groundwater in three sub-basins in the Central Valley of Costa Rica. Uniciencia 32 (1), 43. https://doi.org/10.15359/ru.33-1.4.
Madrigal-Solís, H., Jiménez-Gavilán, P., Vadillo-Pérez, I., Fonseca-Sánchez, A., Calderón-Sánchez, H., Quesada-Hernández, L., Gómez-Cruz, A., 2022. Discriminant model and hydrogeochemical processes for characterizing preferential flow paths in four interconnected volcanic aquifers in Costa Rica. Hydrgeol. J. 30 (8), 2315–2340. https://doi.org/10.1007/s10040-022-02557-7.
Magaña, V., Amador, J.A., Medina, S., 1999. The midsummer drought over Mexico and Central America. J. Climate 12 (6), 1577–1588. https://doi.org/10.1175/1520-0442(1999)012<1577:TMDOMA>2.0.CO;2.
Maldonado, T., Alfaro, E., Fallas-López, B., Alvarado, L., 2013. Seasonal prediction of extreme precipitation events and frequency of rainy days over Costa Rica, Central America, using canonical correlation analysis. Adv. Geosci. 33, 41–52. https://doi.org/10.5194/adgeo-33-41-2013.
Marković, T., Karlović, I., Orlić, S., Kajan, K., Smith, A.C., 2022. Tracking the nitrogen cycle in a vulnerable alluvial system using a multi proxy approach: case study Varaždin alluvial aquifer, Croatia. Sci. Total Environ. 853, 158632 https://doi.org/10.1016/j.scitotenv.2022.158632.
Maurya, J., Pradhan, S.N., Seema, & Ghosh, A. K., 2021. Evaluation of ground water quality and health risk assessment due to nitrate and fluoride in the middle indo-Gangetic plains of India. Hum. Ecol. Risk Assess. Int. J. 27 (5), 1349–1365. https://doi.org/10.1080/10807039.2020.1844559.
McDaniel, P. A., Lowe, D. J., Arnalds, O., & Ping, C. L. (2012). Andisols. En P. M. Huang, Y. Li, & M. E. Sumner (Eds.), Handbook of soil sciences. Vol. 1: properties and processes (2.ª Ed., p. 33.29-33.48).
McMahon, P.B., Chapelle, F.H., 2008. Redox processes and water quality of selected principal aquifer systems. Ground Water 46 (2), 259–271. https://doi.org/10.1111/j.1745-6584.2007.00385.x.
Meghdadi, A., Javar, N., 2018. Quantification of spatial and seasonal variations in the proportional contribution of nitrate sources using a multi-isotope approach and Bayesian isotope mixing model. Environ. Pollut. 235, 207–222. https://doi.org/10.1016/j.envpol.2017.12.078.
MINAE, 2023. *Water statistics and indicators, Costa Rica, 2021 (Estadísticas e indicadores del Agua, Costa Rica, 2021)*. [dataset]. National Information System for integrated water resource management (Sistema Nacional de Información Para la Gestión Integrada del Recurso Hídrico). https://da.go.cr/estadisticas-e-indicadores-del-agua/.
Minet, E.P., Goodhue, R., Meier-Augenstein, W., Kalin, R.M., Fenton, O., Richards, K.G., Coxon, C.E., 2017. Combining stable isotopes with contamination indicators: A method for improved investigation of nitrate sources and dynamics in aquifers with mixed nitrogen inputs. Water Res. 124, 85–96. https://doi.org/10.1016/j.watres.2017.07.041.
MMARN, 2021. *Fertilization of the Coffee Plant (Fertilización del Cafeto)*: United Nations Development Programme (UNDP).
Mora, M.L., Baeza, G., Pizarro, C., Demanet, R., 1999. Effect of calcitic and dolomitic lime on physicochemical properties of a Chilean Andisol. Commun. Soil Sci. Plant Anal. 30 (3–4), 427–439. https://doi.org/10.1080/00103629909370214.
Mora, M.L., Cartes, P., Demanet, R., Cornforth, I.S., 2002. Effects of lime and gypsum on pasture growth and composition on an acid Andisol in Chile, South America. Commun. Soil Sci. Plant Anal. 33 (13–14), 2069–2081. https://doi.org/10.1081/CSS-120005749.
Mora-Alvarado, D.A., Alfaro-Herrera, N., Portuguez-Barquero, C.F., 2017. Estudio sobre la concentración de nitratos en los principales acuíferos del Valle Central de Costa Rica, periodos 1989-2005 y 2006-2015. Rev. Tecnol. Marcha 29 (4), 34. https://doi.org/10.18845/tm.v29i4.3035.
Mora-Alvarado, D., Portuguez, F., 2021. Water for Human Consumption and Sanitation in Costa Rica by 2020: Gaps in Times of Pandemic [Agua para consumo humano y saneamiento en Costa Rica al 2020: Brechas en tiempos de pandemia. Instituto Costarricense de Acueductos y Alcantarillados. https://www.aya.go.cr/transparencia inst/rendicion_cuentas/planesespecificossectorial/agua%20para%20consumo%20humano%20y%20saneamiento%20en%20costa%20rica%20al%202020_%20brechas%20en%20tiempos%20de%20pandemia.pdf.
Nikolenko, O., Jurado, A., Borges, A.V., Knöller, K., Brouyère, S., 2018. Isotopic composition of nitrogen species in groundwater under agricultural areas: A review. Sci. Total Environ. 621, 1415–1432. https://doi.org/10.1016/j.scitotenv.2017.10.086.
Olego, M.Á., Quiroga, M.J., Mendaña-Cuervo, C., Cara-Jiménez, J., López, R., Garzón-Jimeno, E., 2021. Long-term effects of calcium-based liming materials on soil fertility sustainability and Rye production as soil quality indicators on a Typic Palexerult. Processes 9 (7), 1181. https://doi.org/10.3390/pr9071181.
Pérez, W., Alvarado, G.E., Gans, P.B., 2006. The 322 ka Tiribí tuff: stratigraphy, geochronology and mechanisms of deposition of the largest and most recent ignimbrite in the Valle central, Costa Rica. Bull. Volcanol. 69 (1), 25–40. https://doi.org/10.1007/s00445-006-0053-x.
Protti, R., 1986. Geología del flanco sur del volcán Barba. Bol. Vulcanológico Universidad Nacional 17 (23−31).
Ramírez Ch., R., Alfaro M., A., 2002. Mapa de vulnerabilidad hidrogeológica de una parte del Valle Central de Costa Rica. Revi. Geológica América Central 27, 53–60. https://doi.org/10.15517/rgac.v0i27.7804.
Reynolds-Vargas, J., Fraile-Merino, J., 2009. Utilización de isótopos estables en la precipitación para determinar zonas de recarga del acuífero Barva, Costa Rica (Technical Report IAEA-TECDOC-1611. International Atomic Energy Agency, pp. 83–95. https://www-pub.iaea.org/MTCD/publications/PDF/TE_1611s_web.pdf.

Reynolds-Vargas, J., Richter, D.D., Bornemisza, E., 1994. Environmental impact of nitrification and nitrate adsorption in fertilized Andisols in the Valle Central of Costa Rica. Soil Sci. 157, 289–299.

Reynolds-Vargas, J., Fraile-Merino, J., Hirata, R., 2006. Trends in Nitrate Concentrations and Determination of its Origin Using Stable Isotopes (^{18}O and ^{15}N) in Groundwater of the Western Central Valley, Costa Rica. AMBIO: J. Hum. Environ. 35 (5), 229–236. https://doi.org/10.1579/05-R-046R1.1.

Rivett, M.O., Buss, S.R., Morgan, P., Smith, J.W.N., Bemment, C.D., 2008. Nitrate attenuation in groundwater: A review of biogeochemical controlling processes. Water Res. 42 (16), 4215–4232. https://doi.org/10.1016/j.watres.2008.07.020.

Robertson, W., 2021. Septic system impacts on groundwater quality. http://gw-project.org/books/septic-system-impacts-on-groundwater-quality/.

Rojas, V., Barahona, D., Alvarado, G.E., 2017. Geomorfología y petrografía de la colada Ángeles y del cono Monte de la Cruz, volcán Barva, Costa Rica. Rev. Geológica América Central 56, 17–35. https://doi.org/10.15517/rgac.v0i56.29240.

Rütting, T., Boeckx, P., Müller, C., Klemedtsson, L., 2011. Assessment of the importance of dissimilatory nitrate reduction to ammonium for the terrestrial nitrogen cycle. Biogeosciences 8 (7), 1779–1791. https://doi.org/10.5194/bg-8-1779-2011.

Ryan, M.C., Graham, G.R., Rudolph, D.L., 2001. Contrasting nitrate adsorption in Andisols of two coffee plantations in Costa Rica. J. Environ. Qual. 30 (5), 1848–1852. https://doi.org/10.2134/jeq2001.3051848x.

San Martin Ruiz, M., Reiser, M., Kranert, M., 2021. Nitrous oxide emission fluxes in coffee plantations during fertilization: A case study in Costa Rica. Atmosphere 12 (12), 1656. https://doi.org/10.3390/atmos12121656.

Sánchez-Gutiérrez, R., Sánchez-Murillo, R., Esquivel-Hernández, G., Birkel, C., Boll, J., Rojas-Jiménez, L.D., Castro-Chacón, L., 2023. Nitrate legacy in a tropical and complex fractured volcanic aquifer system. J. Geophys. Res. G: Biogeosciences 128 (8), e2023JG007554. https://doi.org/10.1029/2023JG007554.

Shen, H., Rao, W., Tan, H., Guo, H., Ta, W., Zhang, X., 2023. Controlling factors and health risks of groundwater chemistry in a typical alpine watershed based on machine learning methods. Sci. Total Environ. 854, 158737 https://doi.org/10.1016/j.scitotenv.2022.158737.

SINIGIRH, 2018. Statistics and Indicators of Water. Data System for IWRM Indicators May 2017 (Spreadsheet 2.6.2.e1.a.) (Estadísticas e Indicadores del Agua. Sistema datos indicadores para GIRH Mayo 2017 (Hoja de cálculo 2.6.2.e1.a.)). National Information System for Integrated Water Resource Management [Sistema Nacional de Información para la Gestión Integrada del Recurso Hídrico] [Dataset]. http://www.da.go.cr/indicadores-de-la-gestion-del%20%20-recurso-hidrico/.

Subba Rao, N., Dinakar, A., Sun, L., 2022. Estimation of groundwater pollution levels and specific ionic sources in the groundwater, using a comprehensive approach of geochemical ratios, pollution index of groundwater, unmix model and land use/land cover – A case study. J. Contam. Hydrol. 248, 103990 https://doi.org/10.1016/j.jconhyd.2022.103990.

TAHAL, 1990. Master Plan for the Supply of Drinking Water for the Greater Metropolitan Area (Technical Report III). ICosta Rican Institute of Aqueducts and Sewers.

Torres-Martínez, J.A., Mora, A., Knappett, P.S.K., Ornelas-Soto, N., Mahlknecht, J., 2020. Tracking nitrate and sulfate sources in groundwater of an urbanized valley using a multi-tracer approach combined with a Bayesian isotope mixing model. Water Res. 182, 115962 https://doi.org/10.1016/j.watres.2020.115962.

Torres-Martínez, J.A., Mora, A., Mahlknecht, J., Daesslé, L.W., Cervantes-Avilés, P.A., Ledesma-Ruiz, R., 2021. Estimation of nitrate pollution sources and transformations in groundwater of an intensive livestock-agricultural area (Comarca Lagunera), combining major ions, stable isotopes and MixSIAR model. Environ. Pollut. 269, 115445 https://doi.org/10.1016/j.envpol.2020.115445.

Utom, A.U., Werban, U., Leven, C., Müller, C., Knöller, K., Vogt, C., Dietrich, P., 2020. Groundwater nitrification and denitrification are not always strictly aerobic and anaerobic processes, respectively: An assessment of dual-nitrate isotopic and chemical evidence in a stratified alluvial aquifer. Biogeochemistry 147 (2), 211–223. https://doi.org/10.1007/s10533-020-00637-y.

Vystavna, Y., Diadin, D., Yakovlev, V., Hejzlar, J., Vadillo, I., Huneau, F., Lehmann, M.F., 2017. Nitrate contamination in a shallow urban aquifer in East Ukraine: evidence from hydrochemical, stable isotopes of nitrate and land use analysis. Environ. Earth Sci. 76 (13), 463. https://doi.org/10.1007/s12665-017-6796-1.

Xue, D., Botte, J., De Baets, B., Accoe, F., Nestler, A., Taylor, P., Van Cleemput, O., Berglund, M., Boeckx, P., 2009. Present limitations and future prospects of stable isotope methods for nitrate source identification in surface- and groundwater. Water Res. 43 (5), 1159–1170. https://doi.org/10.1016/j.watres.2008.12.048.

Zaryab, A., Nassery, H.R., Knoeller, K., Alijani, F., Minet, E., 2022. Determining nitrate pollution sources in the Kabul plain aquifer (Afghanistan) using stable isotopes and Bayesian stable isotope mixing model. Sci. Total Environ. 823, 153749 https://doi.org/10.1016/j.scitotenv.2022.153749.

Zhang, H., Xu, Y., Cheng, S., Li, Q., Yu, H., 2020. Application of the dual-isotope approach and Bayesian isotope mixing model to identify nitrate in groundwater of a multiple land-use area in Chengdu plain, China. Sci. Total Environ. 717, 137134 https://doi.org/10.1016/j.scitotenv.2020.137134.

Zhang, M., Zhi, Y., Shi, J., Wu, L., 2018. Apportionment and uncertainty analysis of nitrate sources based on the dual isotope approach and a Bayesian isotope mixing model at the watershed scale. Sci. Total Environ. 639, 1175–1187. https://doi.org/10.1016/j.scitotenv.2018.05.239.

Zuo, R., Pan, M., Li, J., Meng, L., Yang, J., Zhai, Y., Xue, Z., Liu, J., Shi, J., Teng, Y., 2021. Biogeochemical transformation processes of iron, manganese, ammonium under coexisting conditions in groundwater based on experimental data. J. Hydrol. 603, 127120 https://doi.org/10.1016/j.jhydrol.2021.127120.